M²HATS

NCAR/EOL ISFS Surface Meteorology and Flux Products Data Report

Prepared by Jacquelyn Witte - ISF Data Manager

Earth Observing Laboratory
In situ Sensing Facility

NATIONAL CENTER FOR ATMOSPHERIC RESEARCH
BOULDER, COLORADO 80307-3000



Table of Contents

M2HATS Principal Investigators 4
EOL ISFS Main Staff 4
Web References 4
Visualization Resources 4
Related Documentation 4
Citations 4
The Dataset 4
The ISFS Platform 5
Acknowledgement 5
Document Version Control 5
Overview 5
Dataset Description 5
5-minute dataset 5
High Rate datasets 6
Site Description 6
Towers 6
Multi-level tower relocation at the beginning of operations 7
Additional Sensors 8
Instrument Set-up and Measurement Description 13
Towers 13
Additional sensors 14
Data Collection and Processing 16
M2HATS NetCDF Variable Naming Convention 17
ISFS netCDF File Conventions 17
Higher Moments 19
A note about flux corrections 20
t0 Trailer Tower Lowering 21
Rain Events 22
Tropical Storm Hilary 23
Data Quality by Instrument 24
Barometers 24
Hygro-thermometer (T, RH) 24
TRH Calibrations 24
Radiometers 27
CSAT 3-D Sonic anemometers 28
Theodolite Geographic Coordinates and Tilt Corrections 30
Sonic Calibrations 33

EC150 Infrared Gas Analyzer (H_2O/CO_2) 34
H_2O 35
CO_2 36
Soils 37
Heat flux, Gsoil 37
Soil Temperature, Tsoil 37
Soil Moisture, Qsoil 38
Soil thermal properties (TP01) 39
Percival2 Ott Disdrometer 39
Data Availability **40**
Minor Data Gaps 41
Appendix A **42**
Appendix B **44**

M2HATS Principal Investigators

Chenning Tong - Clemson University, South Carolina
Shane Mayor - California State University, Chico

EOL ISFS Main Staff

ISFS Lead Scientist: Steven Oncley (Emeritus)
Lead Project Engineer: Chris Roden <croden@ucar.edu>
Data Manager: Jacquelyn Witte <jwitte@ucar.edu>
Software Engineers: Gary Granger, Isabel Suhr, Rick Brownrigg
Technicians: Anthony Wiese, William Nicewonger, Justin Hicks
Associate Scientists: Matthew Paulus, Carol Ruchti

Web References

M2HATS Homepage: https://www.eol.ucar.edu/field_projects/m2hats
ISFS Homepage: https://www.eol.ucar.edu/observing_facilities/isfs
Calculation of long-wave radiation from Hukseflux NR01 thermopile and case temperature: https://www.eol.ucar.edu/content/calculation-long-wave-radiation

Visualization Resources

- NCharts: http://datavis.eol.ucar.edu/ncharts/projects/M2HATS
- M2HATS ISFS Daily Data Statistics and Plots

Related Documentation

ISFS netCDF File Conventions: ISFS netCDF File Conventions
ISFS Guides : https://www.eol.ucar.edu/content/isfs-guides

Citations

If these data are used for research resulting in publications or presentations, please acknowledge EOL and NSF by including the following citations, as appropriate:

The Dataset

NSF NCAR/EOL ISFS Team. 2024. M2HATS: ISFS Surface Meteorology and Flux Products. Version 1.0. UCAR/NCAR - Earth Observing Laboratory. https://doi.org/10.26023/HW9Z-MF0D-NX04. Accessed 06 Mar 2024.

The ISFS Platform

NSF NCAR - Earth Observing Laboratory. (1990). NCAR Integrated Surface Flux System (ISFS). UCAR/NCAR - Earth Observing Laboratory. https://doi.org/10.5065/D6ZC80XJ.

Acknowledgement

Users of EOL data are expected to add the following acknowledgement to all of their publications, reports and conference papers that use those data:

"We would like to acknowledge operational, technical and scientific support provided by NCAR's Earth Observing Laboratory, sponsored by the National Science Foundation."

Document Version Control

Version	Date	Description
1.0	2024-03-06	Initial release
1.1	2024-08-30	Reprocessed datasets with corrected Azimuth angles, and Leica adjustments wrt gravity

Overview

The ISFS system for M2HATS provides surface flux observations at extensive horizontal scales to better characterize the surface layer of the atmospheric boundary layer. These measurements, combined with energy and mass balance observations, will provide benchmarks of the most reliable approaches testing the multi-point Monin-Obukhov similarity hypothesis. M2HATS was operated during the summer of 2023.

Dataset Description

Project Period: 23 July 2023 - 24 September 2023
Dataset Period: 23 July 2023 - 24 September 2023

Center Location: Tonopah, Nevada, USA
Data version: v1.0, Final

5-minute dataset

Data format: netCDF3
File name format: isfs_m2hats_qc_geo_tiltcor_5min_YYYYmmDD.nc

Geographic coordinates: Yes
Tilt adjusted with respect to gravity: Yes
Time resolution: 5-minute

High Rate datasets

Data format: netCDF3

File name format: isfs_m2hats_hr_qc_geo_tiltcor_hr_YYYYmmDD.nc
- Geographic coordinates: Yes
- Tilt corrected anemometers: Yes

File name format: isfs_m2hats_hr_qc_geo_hr_YYYYmmDD.nc
- Geographic coordinates: Yes
- Tilt corrected anemometers: No

Time resolution: - Varies from 0.02 sec to 1 sec depending on the sensor
- Refer to **Appendix B** for a complete list of variables and sampling rates.

Downloadable files from the archive	Type	tar.gz	Untarred
isfs_m2hats_qc_geo_hr_202307.tar.gz, isfs_m2hats_qc_geo_tiltcor_hr_202307.tar.gz	High rate 0.02 - 1 s	34 Gb	72 Gb
isfs_m2hats_qc_geo_hr_202308.tar.gz, isfs_m2hats_qc_geo_tiltcor_hr_202308.tar.gz	High rate 0.02 - 1 s	119 Gb	246 Gb
isfs_m2hats_qc_geo_hr_202309.tar.gz, isfs_m2hats_qc_geo_tiltcor_hr_202308.tar.gz	High rate 0.02 - 1 s	95 Gb	192 Gb
isfs_m2hats_qc_geo_tiltcor_5min.tar.gz	5 min averages	141 Mb	188 Mb

Site Description

Towers

- 5 meter towered horizontal array
  - 50 x 4.5m towers aligned in a horizontal array spanning roughly 250 meters long with 5m spacing between towers. Sensors were mounted nominally at 4m. Refer to **Table 1** for sensor location and heights.
- Multi-level towers
  - 1 x 6m Rohn tower
  - 1 x 30m Trailer tower

Refer to **Schematic 1** for a top-down view of the final site placement relative to the ISS and PI base operations. **Figure 1** maps each site's placement based on a QGIS georeferenced map. **Photos 1A-C** give a side view of the array and towers.

50 - 4.5m flux towers were set-up as a horizontal array with sensors mounted at a nominal height of 4m. These towers are named from t0p (west) to t49 (east) (refer to **Schematic 1**).

The two additional towers (a 6m and 30m multi-level tower) were located at the east end of the fifty tower array. These towers had sensors mounted at multiple heights to provide profiles of winds, H_2O/CO_2, pressure, temperature, and RH from 0.5m to 30m at discrete heights. Together, the two multiple sensor towers have been given the single site name, t0, and are uniquely identified by the height of each sensor. This is to combine the measurements into vertical profiles from 0.5m to 28m from the two towers. The towers were split into the short and tall tower to avoid the influence of the tall tower's base superstructure on the airflow sensed by the sensors below 7m. **Table 1** gives the final location and height of each tower determined by the Leica surveying equipment.

Note that the GPS coordinates listed for sites t0p through t18 had to be manually adjusted because of the way in which the Leica scans were conducted. The Leica scans were performed from two different reference positions: t0p to t18 at one Leica reference, and t19-t49 from another reference. This unknowingly caused a discontinuity of about 1 m difference between sites t18 and t19. For the GPS coordinates of sites t0p through t18 in **Table 1**, an offset (Longitude offset: -1.311E-05 degrees, Latitude offset: -6.920E-06 degrees) was applied to correct for this Leica reference difference.

Note that the latitude, longitude, and altitude in the netCDF file are based on the GPS samples from the DSM data logger. On the array, there was a data logger on every 3rd tower starting at site t0. These GPS listings in the netCDF are not very precise and Leica-based GPS listings in **Table 1** are more precise. However even **Table 1** does not reflect the actual precision of the 50 tower array. The array was precisely measured and constructed along a straight line. Each tower was positioned +/- 5cm (off the centerline), with a precise lateral tower spacing of 5 meters +/- 5cm.

Multi-level tower relocation at the beginning of operations

At the start of operations (23 July), the 30m trailer tower was initially located over 1 km southwest of the 5m horizontal array close to the ISFS, ISS and REAL base trailers (refer to **Schematic 1**) and it was determined that the difference in vegetation and terrain slope in the locations of the 6m and 30m towers were significant enough to cause a discontinuity in the combined wind speed and temperature profiles (**Figure 2**). On 25 July the trailer tower was moved to its final location ~125m east northeast of array. The 6m multi-level tower was moved on 27 July ~100m east of the array. The distortion was minimized further by extending the boom at 7m trailer tower on 31 July.

Timeline of the relocation of the 6m and 30m towers

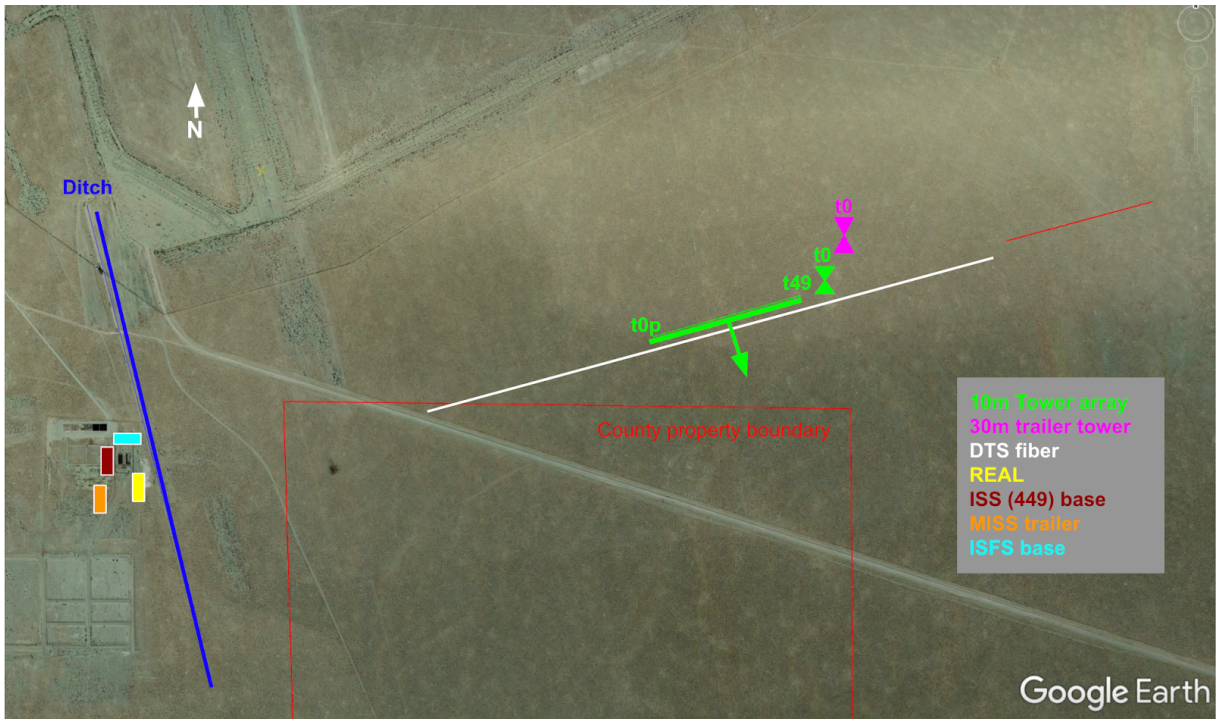
- July 23 start of ops

- July 25 moved 30m trailer tower (~125m east northeast of array)
- July 27 moved 6m Rohn tower closer to the trailer tower (100m east of array)
- July 27 - t0p was set-up on the western end of the array. Data collection started July 28 04:42:30 UTC.
- July 31 add longer boom at 7m trailer tower

Because of the movement of sites and sensors during the beginning of operations, it is not recommended to use profiles of wind measurements (site name t0) prior to 31 July 2023.

Additional Sensors

- Soil sensors were placed at three sites - t2, t23, and t49 - to span the center and edges of the horizontal array.
- Two radiometers were set up, one at each end of the array - t2 and t49. A wetness sensor was coupled to each radiometer to filter incidences of moisture on the sensor dome, i.e. dew, rain, or snow.



Schematic 1. Schematic rendering of horizontal array and 30m trailer tower, relative to the ISS and PI base operations.

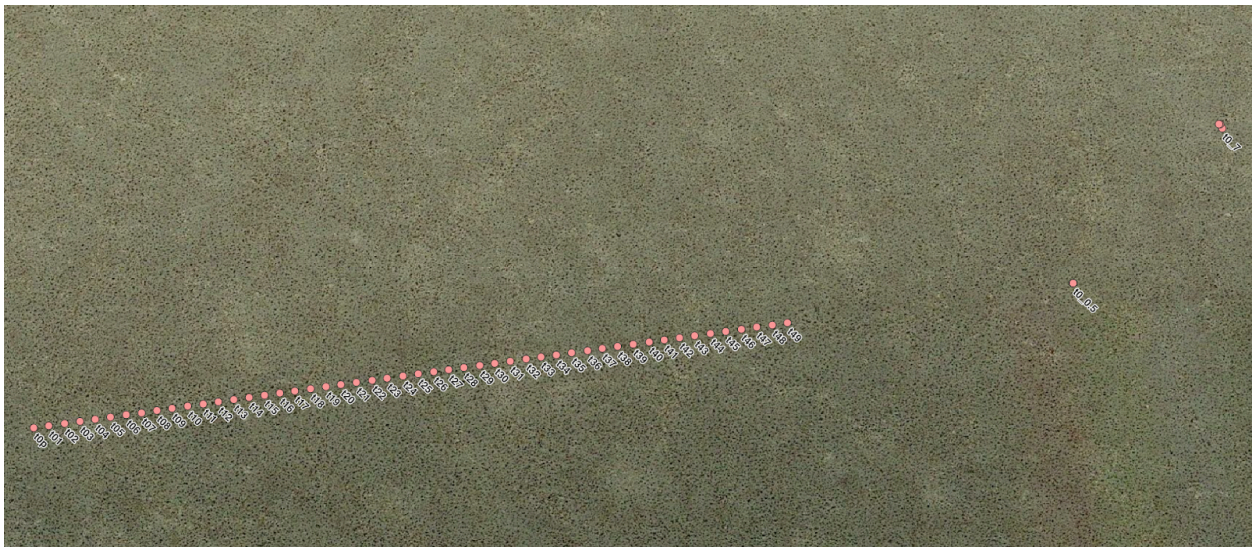


Figure 1. QGIS map of each site.



Photo 1A. View of a section of the horizontal array at sunset. 3D sonic anemometers are mounted facing towards the south.



Photo 1B. View of t0 6m tower with Temperature, RH, P, H_2O/CO_2 gas analyzers, and 3D sonic sensors mounted at 0.5m, 1m, 2m, 3m, and 4m.



Photo 1C. View of t0 30m tower with Temperature, RH, P, H_2O/CO_2 gas analyzers, and 3D sonic sensors mounted at 7m, 15m, and 28m.

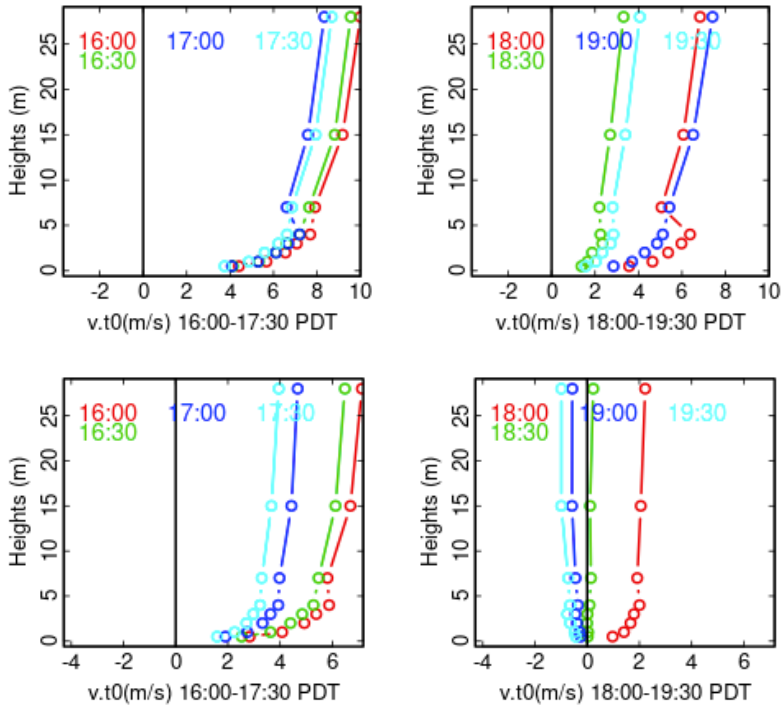


Figure 2. Top plots are the v component profiles from t0 towers on 23 July before the relocation of the trailer tower. The bottom plots were taken on 1 August after the move to the east of the array and the extension of the 7m boom on the 30 trailer tower.

Table 1. Sites and locations. Note that the site name is the netCDF sitename definition. Locations were determined by the Leica surveying equipment (theodolite).

(A) Horizontal array location and heights of mounted sensors determined by the theodolite.

Site name	Height (m)	Longitude (deg)	Latitude (deg)
t0p	4.484	-117.0742621	38.04264114
t01	4.524	-117.0742073	38.04264879
t02	4.539	-117.0741494	38.04265703
t03	4.562	-117.0740934	38.04266465
t04	4.637	-117.0740379	38.04267236
t05	4.505	-117.0739823	38.04268031
t06	4.577	-117.0739246	38.04268885
t07	4.476	-117.0738686	38.04269536
t08	4.477	-117.0738127	38.04270436
t09	4.435	-117.0737576	38.04271223
t10	4.435	-117.0737003	38.04272029

t11	4.382	-117.0736437	38.04272789
t12	4.445	-117.0735887	38.04273585
t13	4.368	-117.0735322	38.04274399
t14	4.275	-117.0734764	38.04275169
t15	4.268	-117.0734201	38.04275979
t16	4.25	-117.0733642	38.04276774
t17	4.18	-117.0733096	38.0427752
t18	4.307	-117.0732521	38.04278321
t19	4.241	-117.073196	38.04279101
t20	4.196	-117.0731418	38.04279866
t21	4.223	-117.0730852	38.04280654
t22	4.234	-117.0730274	38.0428141
t23	4.19	-117.0729731	38.04282168
t24	4.241	-117.0729152	38.04282979
t25	4.192	-117.0728595	38.04283755
t26	4.19	-117.0728028	38.04284525
t27	4.262	-117.0727484	38.04285281
t28	4.236	-117.0726928	38.0428604
t29	4.21	-117.072635	38.04286808
t30	4.344	-117.0725804	38.04287555
t31	4.34	-117.0725238	38.0428834
t32	4.326	-117.0724658	38.0428916
t33	4.417	-117.0724114	38.04289897
t34	4.393	-117.0723555	38.04290635
t35	4.399	-117.072300	38.04291432
t36	4.424	-117.0722415	38.04292203
t37	4.421	-117.072188	38.04292989
t38	4.303	-117.0721322	38.04293735
t39	4.384	-117.0720752	38.04294517
t40	4.391	-117.0720169	38.04295332
t41	4.347	-117.071962	38.04296114
t42	4.416	-117.071906	38.04296853
t43	4.435	-117.071851	38.04297646
t44	4.413	-117.0717935	38.04298414
t45	4.439	-117.0717377	38.04299194
t46	4.422	-117.0716806	38.04299969
t47	4.356	-117.0716247	38.04300773

t48	4.416	-117.0715677	38.04301529
t49	4.406	-117.0715126	38.04302335

(B) Site t0 multi-level tower location and heights of mounted sensors determined by the theodolite.

Site	Height (m)	Latitude (deg)	Longitude (deg)
t0_0.5	0.615	-117.0704707	38.0431674
t0_1	1.166	-117.0704705	38.04316741
t0_2	2.114	-117.0704705	38.04316738
t0_3	3.016	-117.0704704	38.04316738
t0_4	4.198	-117.0704701	38.04316737
t0_7	6.894	-117.0699262	38.04373068
t0_15	15.453	-117.0699341	38.0437454
t0_28	28.551	-117.0699382	38.04374603

Instrument Set-up and Measurement Description

Towers

- 50 x 4.5 meter Rohn towers
  - 1 level (~4m)
    - CSAT 3D sonic anemometer
    - Every third tower
      - IRGA EC150 H_2O/CO_2 gas analyzer
      - Temperature and RH
      - Nanobarometer

- 1 x 6 meter Rohn tower
  - 5 levels (0.5m, 1m, 2m, 3m, 4m)
    - CSAT 3D sonic anemometer
    - IRGA EC150 H_2O/CO_2 gas analyzer
    - Nanobarometer
  - 4 levels of Temperature and RH (1m, 2m, 3m, 4m)
  - 4 levels of PI supplied Hot Film sensors (0.5m, 1m, 2m, 4m)

- 1 x 30 meter trailer tower
  - 3 levels (7m, 15m, 28m)
    - CSAT 3D sonic anemometer
    - IRGA EC150 H_2O/CO_2 gas analyzer
    - Temperature and RH
    - Nanobarometer

Additional sensors

- 3 sets of soil sensors located at sites t2, t23, and t49
- 2 NR01: 4 component radiometers at sites t2 and t49
- 1 disdrometer at the 30m tower

All 3D sonic anemometers and coupled gas analyzers were mounted facing south (see **Photo 1**). The nanobarometer quad-disk inlets were mounted on the 3D sonic booms slightly behind and offset from the sonic. The Temperature, RH, sensors were mounted 120 degrees from the anemometers to the east to minimize distortion around the anemometers.

ISFS used three models of CSAT 3D sonics that recorded measurements at variable rates:

- CSAT3A with IRGA EC 150 gas analyzer - Sample rate set to 60 sample/s.
- CSAT3B - Sample rates can be set to 10, 20, 50, or 100 samples/s. The rate for M2HATS was set to 50 samples/s to closely match that of the CSAT3A's.
- CSAT3 - Sample rate default is 30 samples/s.

Attempts were made to space the various CSAT models evenly. Refer to **Appendix A** for a table of CSAT models used at each site. The 6m and 30m towers used the CSAT3A model with a EC150 gas analyzer.

The standard 5-min ISFS products include measurements from the sensors listed in **Table 2**. High rate data contain measurements from Table 2 A and B.

Table 2. ISFS sensors and description. Measurements from (A) and (B) are provided in both the 5-minute and high rate datasets. (C) are non-towered sensors that are provided in the 5-minute dataset only due to the slow sample rate. Refer to **Appendix B** for a complete list of all high rate variables and sample rates.

(A) Horizontal Array, t0p-t49

Instrument	Manufacturer - Model	Sites	Samples/s
3D sonic anemometer	Campbell Scientific CSAT3	Refer to Appendix A	30
	Campbell Scientific CSAT3A**	Refer to Appendix A	60
	Campbell Scientific CSATB	Refer to Appendix A	50

H_2O/CO_2 Open-path InfraRed Gas Analyzer (IRGA)	Campbell Scientific (combination of EC100 and EC150)	Every 3rd tower starting at site t2	60
Hygro-thermometer	Sensirion SHT85		1
Nanobarometer	Paroscientific 6000		20

**With the optional CSAT3A sonic anemometer head to couple with the IRGA EC150.

(B) Multi-level towers, t0.

Instrument	Manufacturer	Heights (m)	Samples /s
3D sonic anemometer	Campbell Scientific CSAT3A	0.5, 1, 2, 3, 4, 7, 15, 28	60
H_2O/CO_2 Open-path InfraRed Gas Analyzer (IRGA)	Campbell Scientific (combination of EC100 and EC150)		
Hygro-thermometer	Sensirion SHT85		1
Nanobarometer	Paroscientific 6000		20

(C) Additional Sensors

Instrument	Manufacturer	Site	Samples/s
Wetness	Decagon	t2, t49	0.2
Integrated Net Radiometer	4-component Hukseflux NR01	t2, t49	0.2
Soil temperature profile sensor	NCAR 4-level Tsoil	t2, t23, t49	0.2
Soil thermal properties	Hukseflux TP01	t2, t23, t49	0.2
Soil Moisture	Meter EC-5	t2, t23, t49	0.2
Heat flux plate	REBS HFT	t2, t23, t49	0.2
Disdrometer	OTT Parsivel2	30m tower	0.02

Data Collection and Processing

All sensors were sampled independently with a Linux-based Data System Module, or DSM. Data were stored directly onto USB sticks provided for every DSM. At M2HATS, all DMSs used a shared ubiquiti wireless network to transmit raw data in real time to a server at the ISFS base trailer for local storage, with added periodic back-ups to servers at EOL. Data acquisition and processing were performed by the NIDAS software developed at EOL.

NIDAS (NCAR In-situ Data Acquisition Software) is a linux-based software that handles the data processing for all ISFS measurement systems. Each sensor is sampled independently. A time tag is assigned to each sample at the moment it is received, based on a system clock synchronized to GPS time. Minimal data interpretation is performed to differentiate individual messages from a sensor, assembling the data exactly as it was received into a sample, with the associated time-tag and an identifier of the sensor and data system. The concatenated stream of samples from all sensors is then passed on for archival and further processing.

NIDAS reads a series of configuration and calibration files that contain pertinent sensor metadata and, more importantly, any input variables that are to be applied to the data either during operations or in post-processing. NIDAS will also apply quality control flags and filters, and thresholds. To generate the 5-minute average and high rate datasets, NIDAS reads the variables from the raw information, applies calibrations and quality control filters, generates 5-minute averages for those datasets, then writes the variables to netCDF.

- Further introduction to NIDAS and access to the software can be found on its GitHub Wiki.
- NIDAS version used to process datasets is v1.2.1-8

M2HATS NetCDF Variable Naming Convention

Data files are provided in netCDF3 format. Research parameters contained in the 5-minute and high rate data are provided below. **Table 3** lists the relevant research variables.

ISFS netCDF File Conventions

Refer to the ISFS netCDF File Conventions for a readme guide to understanding how ISFS netCDF data files are constructed and how standard variables are defined.

Also, please note that 5-minute averaging often is insufficient to capture all of the scales of turbulence contributing to the total flux, especially in unstable (daytime) conditions. We recommend averaging longer, which can easily be done from the 5-minute average data, using the procedure described in combining short-term moments.

ISFS Variable naming convention follows the convention of <variable>_<height>_<site name>. For example, spd_15m_t0 refers to the 3D anemometer wind speed at 15 meters at site t0, Tsoil_3_1cm_t23 refers to soil temperature buried 3.1 cm at site t23, and P_4m_t35 refers to pressure from the nanobarometer at the t35 array tower:

```
float spd_15m_t0(time) ;
            spd_15m_t0:_FillValue = 1.e+37f ;
            spd_15m_t0:long_name = "CSAT3 horizontal wind speed" ;
            spd_15m_t0:short_name = "spd.15m.t0" ;
            spd_15m_t0:units = "m/s" ;
```

```
float Tsoil_3_1cm_t23(time) ;
            Tsoil_3_1cm_t23:_FillValue = 1.e+37f ;
            Tsoil_3_1cm_t23:long_name = "Soil temperature 3.1cm" ;
            Tsoil_3_1cm_t23:short_name = "Tsoil.3.1cm.t23" ;
            Tsoil_3_1cm_t23:units = "degC" ;

float P_4m_t35(time) ;
            P_4m_t35:_FillValue = 1.e+37f ;
            P_4m_t35:long_name = "Barometric Pressure, Paroscientific
6000" ;
            P_4m_t35:short_name = "P.4m.t35" ;
            P_4m_t35:units = "mb" ;
            P_4m_t35:counts = "counts_4m_t35_3" ;
```

Table 3. ISFS Instruments and measurements.

Instrument or Type	Variable Name	Unit	Measurement
CSAT 3D sonic anemometer	u	m/s	Wind U component
	v	m/s	Wind V component
	w	m/s	Wind W component
	dir	deg	Wind direction
	spd	m/s	Wind speed
	ldiag	-	diagnostic 0=OK
	tc	C	Virtual air temp from speed of sound
EC150 InfraRed Gas Analyzer	h2o	g/m^3	Water vapor density
	co2	g/m^3	CO_2 density
	irgadiag	-	diagnostic, 0=ok
	Pirga	mb	IRGA pressure
	Tirga	C	IRGA temperature
Sensirion SHT85	T	C	Air temperature
	RH	%	Relative humidity

	Rfan	rpm	TRH aspiration fan speed
Barometer	P	mb	Air pressure
Radiometers: NR01	Rsw.in, Rsw.out	W/m^2	Incoming, outgoing shortwave
	Rpile.in, Rpile.out	W/m^2	Incoming, outgoing thermopile
	Tcase	C	Case temperature
	Wetness	V	Leaf wetness
Power	Icharge	mA	Charging current
	Iload	mA	Load current
	Vbatt	V	Battery voltage
GPS	GPSnsat	-	Number of GPS satellites tracked
	GPSstat	-	GPS receiver status: 1=OK, 0=warning
	Stratum	-	Status of time service (1 is best)
	Timeoffset	µs	Clock offset: system-reference
	GPSdiff	s	
Soils	Tsoil	C	Soil temperature
	Qsoil	m^3/m^3	Soil moisture
	Gsoil	W/m^2	Soil Heat Flux
	Lambda	W/m/K	Soil thermal conductivity
	Tau63	s	Time to decay to 37% of Vpile
	Vpile	V	Thermopile after heating
	Vheat	V	Heater voltage
Parsival2 Ott disdrometer	Rainr	mm/h	Rain rate
	Vis	m	Visibility (WRT rain only, not fog)
	N	-	Number of particles

Higher Moments

We provide a long list of 2nd and 3rd moments among the winds, H_2O, and CO_2. They follow the naming convention:

2nd moment: varname_varname__height_sitename

3rd moment: varname_varname_varname__height_sitename

For example,

```
float u_w__7m_t0(time) ;
            u_w__7m_t0:_FillValue = 1.e+37f ;
            u_w__7m_t0:long_name = "2nd moment" ;
            u_w__7m_t0:short_name = "u\'w\'.7m.t0" ;
            u_w__7m_t0:units = "(m/s)^2" ;
            u_w__7m_t0:counts = "counts_7m_t0" ;

float w_w_tc__0_5m_t0(time) ;
            w_w_tc__0_5m_t0:_FillValue = 1.e+37f ;
            w_w_tc__0_5m_t0:long_name = "3rd moment" ;
            w_w_tc__0_5m_t0:short_name = "w\'w\'tc\'.0.5m.t0" ;
            w_w_tc__0_5m_t0:units = "(m/s)^2 degC" ;
            w_w_tc__0_5m_t0:counts = "counts_0_5m_t0" ;

float v_h2o__4m_t41(time) ;
            v_h2o__4m_t41:_FillValue = 1.e+37f ;
            v_h2o__4m_t41:long_name = "2nd moment" ;
            v_h2o__4m_t41:short_name = "v\'h2o\'.4m.t41" ;
            v_h2o__4m_t41:units = "m/s g/m^3" ;
            v_h2o__4m_t41:counts = "counts_4m_t41_1" ;
```

Refer to the ISFS netCDF document which provides further detail on the ISFS instruments and their parameters, the netCDF naming convention, time sampling, and attributes.

A note about flux corrections

The calculation of certain fluxes is a bit more involved than just the covariance, due to the spatial separation of some sensors, the sensitivity of the sonic anemometer temperature to humidity, and density effects. For example, when calculating sensible and latent heat fluxes one should apply corrections to the following variables:

Variable name	Quantity Measured	unit	Correction
w_tc__	Covariance of vertical velocity with virtual air temperature from speed of sound	m/s degC	The correction of measured sonic temperature for the effect of moisture (Schotanus et al., 1983, Kaimel and Gaylor, 1991)

w_h2o__	Covariance of vertical velocity with humidity	m/s g/m^3	The “WPL" correction of vertical flux of water vapor density (Webb et al., 1980)
w_co2__	Covariance of vertical velocity with carbon dioxide	m/s g/m^3	The correction for the spatial separation of the EC150 and CSAT3 (Horst and Lenschow, 2009)

A guide of how one can make above corrections can be found here: https://www.eol.ucar.edu/content/corrections-sensible-and-latent-heat-flux-measurements

References

Schotanus, P., Nieuwstadt, F. & De Bruin, H. Temperature measurement with a sonic anemometer and its application to heat and moisture fluxes. Boundary-Layer Meteorol 26, 81–93 (1983). https://doi.org/10.1007/BF00164332.

Kaimal, J.C., Gaynor, J.E. Another look at sonic thermometry. Boundary-Layer Meteorol 56, 401–410 (1991). https://doi.org/10.1007/BF00119215.

Webb, E.K., G.I. Pearman, and R. Leuning. Correction of flux measurements for density effects due to heat and water vapor transfer. Quart. J. Roy. Meteorol. Soc., 106, 85-100 (1980). https://doi.org/10.1002/qj.49710644707.

Horst, T.W., Lenschow, D.H. Attenuation of Scalar Fluxes Measured with Spatially-displaced Sensors. Boundary-Layer Meteorol 130, 275–300 (2009). https://doi.org/10.1007/s10546-008-9348-0.

t0 Trailer Tower Lowering

Throughout the project, there were periods when the 30m trailer tower was lowered for sensor maintenance. **Table 4** gives a list of those time periods. Data from all sensors on t0 tower were removed during the time periods listed below.

Table 4. Periods where the 30m trailer tower was lowered for maintenance. Links are to the ISFS M2HATS wiki home page blog posts.

t0 Tower Moves/Lowers/Battery Swaps	Start Move	End move
1st Lower of the Tower	2023-07-24 10:30 PDT	2023-07-24 11:30 PDT
1st Move Location	2023-07-25 10:00 PDT	2023-07-25 16:00 PDT
2nd Lowering the Tower	2023-07-31 12:30 PDT	2023-07-31 17:30 PDT
Battery Swap	2023-09-03 07:45 PDT	2023-09-03 10:20 PDT
3rd Lowering the Tower	2023-09-04 12:00 PDT	2023-09-04 13:30 PDT

4th Lowering the Tower	2023-09-11 10:30 PDT	2023-09-11 11:50 PDT
Battery Swap again	2023-09-20 00:00 PDT	2023-09-20 08:30 PDT

Rain Events

Rain events play a role in the data QC process. **Table 5** is a list of events gathered from various sensor data including distrometer, RH, and wetness sensors.

Table 5. A list of rain events determined by the disdrometer, H_2O gas analyzer, T, RH

Rain Events	Start Rain	End Rain
Long Rain 7/24 AM	2023-07-24 00:50 PDT	2023-07-24 03:00 PDT
Short Rain 7/24 AM	2023-07-24 08:30 PDT	2023-07-24 09:30 PDT
Short Rain 7/24 PM	2023-07-24 17:40 PDT	2023-07-24 18:40 PDT
Short Rain 8/2 AM	2023-08-02 02:30 PDT	2023-08-02 03:40 PDT
Rain only detect by OTT 8/10 PM	2023-08-10 18:20 PDT	2023-08-10 19:20 PDT
Very Short Rain 8/13 AM	2023-08-13 10:55 PDT	2023-08-13 11:20 PDT
Tropical Storm Hilary 8/20	**2023-08-19 19:00 PDT**	**2023-08-21 11:00 PDT**
Longer Rain 8/22	2023-08-22 00:30 PDT	2023-08-22 08:00 PDT
Longer Rain 8/25	2023-08-25 02:30 PDT	2023-08-25 04:30 PDT
Longer Rain 9/2	2023-09-02 02:30 PDT	2023-09-02 03:30 PDT
Long Evening Rain 9/3	2023-09-03 16:00 PDT	2023-09-03 21:00 PDT
Short Rain 9/9 AM	2023-09-09 08:30 PDT	2023-09-09 09:30 PDT
Short Rain 9/9 AM	2023-09-09 19:05 PDT	2023-09-09 19:40 PDT
Short Rain 9/10 AM	2023-09-10 02:25 PDT	2023-09-10 03:40 PDT
Short Rain 9/10 AM	2023-09-10 06:30 PDT	2023-09-10 07:15 PDT
Short Rain 9/10 later	2023-09-10 10:30 PDT	2023-09-10 13:00 PDT
Longer Rain 9/12	2023-09-12 19:00 PDT	2023-09-12 20:00 PDT
Very Long Rain 9/13	2023-09-13 15:50 PDT	2023-09-13 20:30 PDT
Last 9/20 rain	2023-09-20 22:00 PDT	2023-09-20 23:30 PDT

Tropical Storm Hilary

From 19 - 21 August 2023 the National Weather Service issued a warning alert for Hurricane Hilary that strengthened into a Category 4 hurricane and tracked west-northwestward in the eastern North Pacific Ocean off the west coast of Mexico early Aug. 18. Hilary weakened into a tropical depression as it tracked generally northward across southern California and Nevada through Aug. 21 (**Photo 2**), before dissipating over southeastern Oregon early Aug. 22. During most of the 19-21 August period many sensors were offline due to lack of power to the towers supplied by solar panels. Staff were able to do the following maintenance, post Hilary, on 21 Aug.

21 August maintenance

- **30m trailer tower** - Replaced the batteries and power cycled the data logger to restore data collection and power the beacon.
- **DSM offline at sites t1 and t23**. The data logger was power cycled to bring the data back online.
- **Site t23** - Replaced the victron that was waterlogged from the sustained severe rainfall. Power cycled the soil mote which was offline.

23 August maintenance

- **Sites t1 and t22** - Replaced bad CSAT 3D sonic anemometers. Note that **t1** was replaced with a CSAT3A sonic (refer to **Appendix A**).
- **Site t41** - Replaced the TRH casing.



Photo 2. Image of the array and tower post Hurricane Hilary on 21 August 2023.

Data Quality by Instrument

ISFS performed data quality checks on all sensors. Below we provide summaries of the QC workflow for each sensor.

Barometers

The Paroscientific nanobarometers were connected to NCAR-built quad-disk probes, based on the design by Nishiyama and Bedard (1998), All pressure sensors worked as expected. No problems were found during QC processing for these sensors and none were replaced during operations. Differences in the average pressures are due to the station elevation specifically for the t0 tall tower.

Data Notes:

- Missing data occurs when the t0 tower is lowered or moved, and you can see those events in the t0 tower movements from **Table 4**.

Hygro-thermometer (T, RH)

The fan speeds in the sensor housings were collected and used as an indicator that the ventilation fans were functioning as expected. In general, the measurements were fairly stable, however, a few casings and sensors were replaced. See data notes below.

Data Notes:

- 23 August: TRH casing at site t41 was replaced.
- 25 August: Replaced the TRH housing at t47, which was reading Rfan values ~2500.
- 11 September: Replaced a bad TRH sensor at the 30 m trailer tower at 28 m.

TRH Calibrations

Calibrations were performed on the TRH sensors in the EOL Calibration Laboratory : https://www.eol.ucar.edu/research-development/calibration-laboratory/calibration-laboratory-resources.

Temperatures are calibrated using Fluke 7060 oil baths, and relative humidity is calibrated using a Thunder Scientific model 2900 Humidity Generator. The temperature sensors are calibrated over a range from -20 to 45 °C in 5 °C steps, and are referenced against a standard platinum resistance thermometer (SPRT) interfaced to a Fluke 1594A Super Thermometer. A typical temperature calibration is shown below in **Figure 3**. The red line with blue dots shows the sensor value minus the reference temperature and is expected to stay within the +/- 0.1 °C bounds.

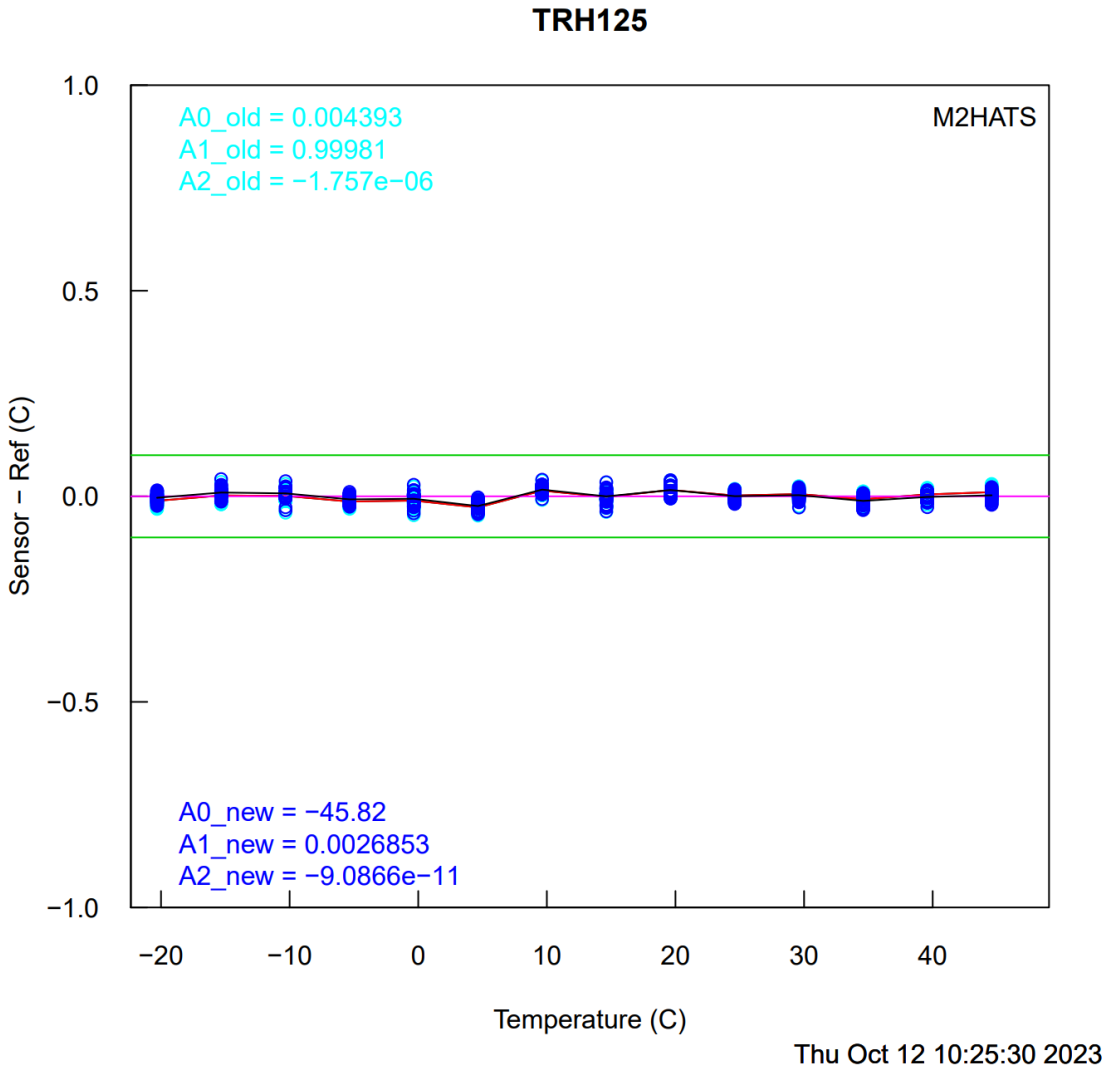


Figure 3. Post-calibration of Temperature plot for TRH sensor 125 (site t0 mounted at 0.5 m) over -20 to 45 ºC in 5 ºC steps. The green lines outline the +/- 0.1 ºC error lines.

The relative humidity calibration is performed at three constant temperatures (0ºC, 20ºC, and 40ºC), with the relative humidity varying from 10 to 90 % RH for each temperature step. To remove the RH hysteresis effect, the RH chamber is programmed to slowly increase from 10% to 90% (we avoid 100% RH to inhibit condensation) then decrease back down to the 10% RH. This calibration process takes three days to complete. Eight RH probes can be calibrated at a time. An example of a RH calibration plot is shown in **Figure 4**.

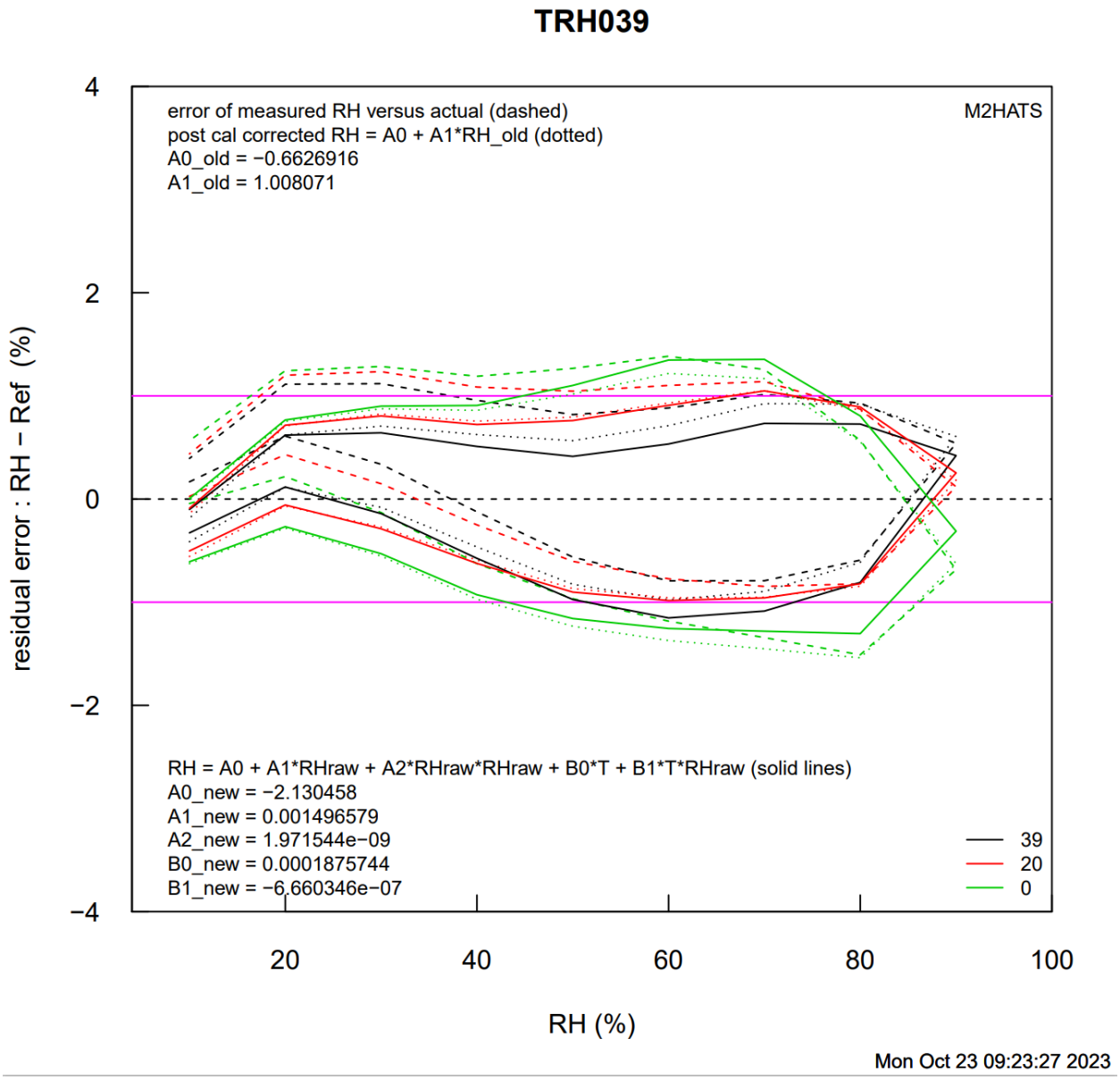


Figure 4. Post-calibration of RH for TRH sensor 039 (site t0 mounted at 1m) at constant temperatures (0°C-green, 20°C-red, and 40°C-black). The curved shape is the result of hysteresis of the RH sensor while measuring the increase then decrease of the known RH source at each temperature. The difference between the upper and lower bounds of the curve defines the hysteresis effect. Dotted lines are the percent residual error relative to a known source of RH before calibration. The solid lines are the adjustments to the fit to reduce the error to within 1%. The final calibrated fits are the solid lines and fits to the average of post-calibrations are provided on the bottom left with additional terms to the fit equations that accounts for the temperature dependence.

Pre-calibrations were completed in April and May, 2022. The pre-calibration process determines coefficients for both temperature and RH for each probe. These coefficients are programmed into the TRH probes, and then the post calibration process verifies that the probe's temperature and RH profile did not shift over the course of the project. All humidity sensors were calibrated to within ± 1% accuracy and all temperature probes were calibrated to within the expected error of ± 0.1°C. Post-calibrations were completed by November 2023.

Post calibration of all temperature probes verified that they were within the expected error of ± 0.1°C. No temperature corrections were applied. Post calibration of the RH sensors verified that all sensors (with the exception of those noted below) were within the expected error of 1% RH (excluding the manufacturer specified ~1% hysteresis error). The following RH sensors showed a greater uncertainty based on post calibrations. TRH sensors 40, 57 and 106 were within 2% RH and sensors 25 and 69 were within 3% RH. For all of these sensors the uncertainties were greater at lower temperatures (0 °C) and at higher relative humidities (70 - 90% RH).

Radiometers

NR01 radiometers were mounted on tripods at nominal heights of 2m. A wetness sensor was attached close to the sensors to record moisture levels.

Radiometer data have been filtered for

- Spikes
- Moisture on the lens due to dew or precipitation as measured by the wetness sensors mounted on the NR01 radiometer.

We used the wetness sensor at t49 to filter for moisture on the radiometer lenses. We used a threshold of wetness > 0.265 V. While this should remove most periods of moisture from dew or precipitation on the radiometers, this is only a first-order correction and may not capture all such events.

Refer to **Figure 11** for final data availability after quality checks for the ISFS-controlled sensors. Calculations of long-wave radiation using the Rpile and Tcase variables as described here: https://www.eol.ucar.edu/content/calculation-long-wave-radiation.

Data notes:

30 July - 07 August: It was discovered that the incoming shortwave radiation at site t2 (variable name = Rsw.in.t2) flatlined at 1028 W/m^2. The response of the Rsw.in signal was higher than the input range of the A/D count. We changed the gain setting on the NR01's A/D for the Rsw.in channel to compensate for this gain change in computing voltages, so the resultant range was extended to 1037 W/m^2, similar to the NR01 set-up at site t49 (1038 W/m^2 max).

CSAT 3-D Sonic anemometers

CSAT3 sonic anemometers were used for turbulence measurements on all towers.

Data notes

An analysis of w'w' across the array confirms that the different models of sonics see different amounts of variance (**Figure 5**). There is good agreement within each type. Variances from the CSAT3As are the highest, CSAT3Bs are lower by about 5%, and CSAT3s even lower by about 15%. This is the order of the sampling rate, and thus the bandwidth.

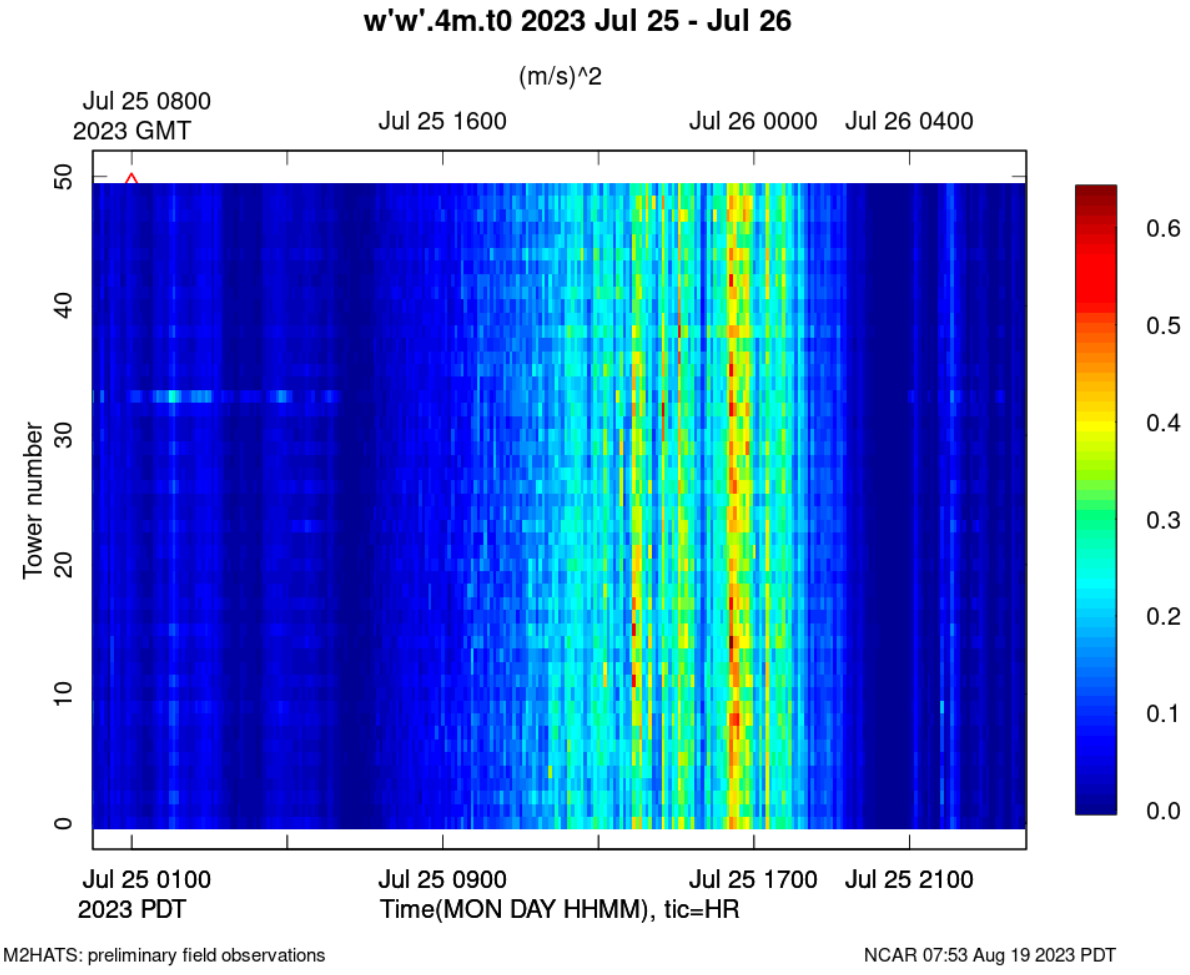


Figure 5. Preliminary plot of w'w' across the horizontal array of 3D sonic anemometers for 25 July. Daily plots of w'w' have been generated for the project and can be accessed at https://archive.eol.ucar.edu/docs/isf/projects/M2HATS/isfs/qcdata/

At the beginning of the project there were noticeable kinks in the trailer tower profiles of 3D sonic winds that varied by day and time (**Figure 6**). This has been mitigated somewhat by extending the 7m boom from 5m to 10m away from the trailer tower on 31 July, arguing that blockage by the tower might reduce the measured winds (even upstream).

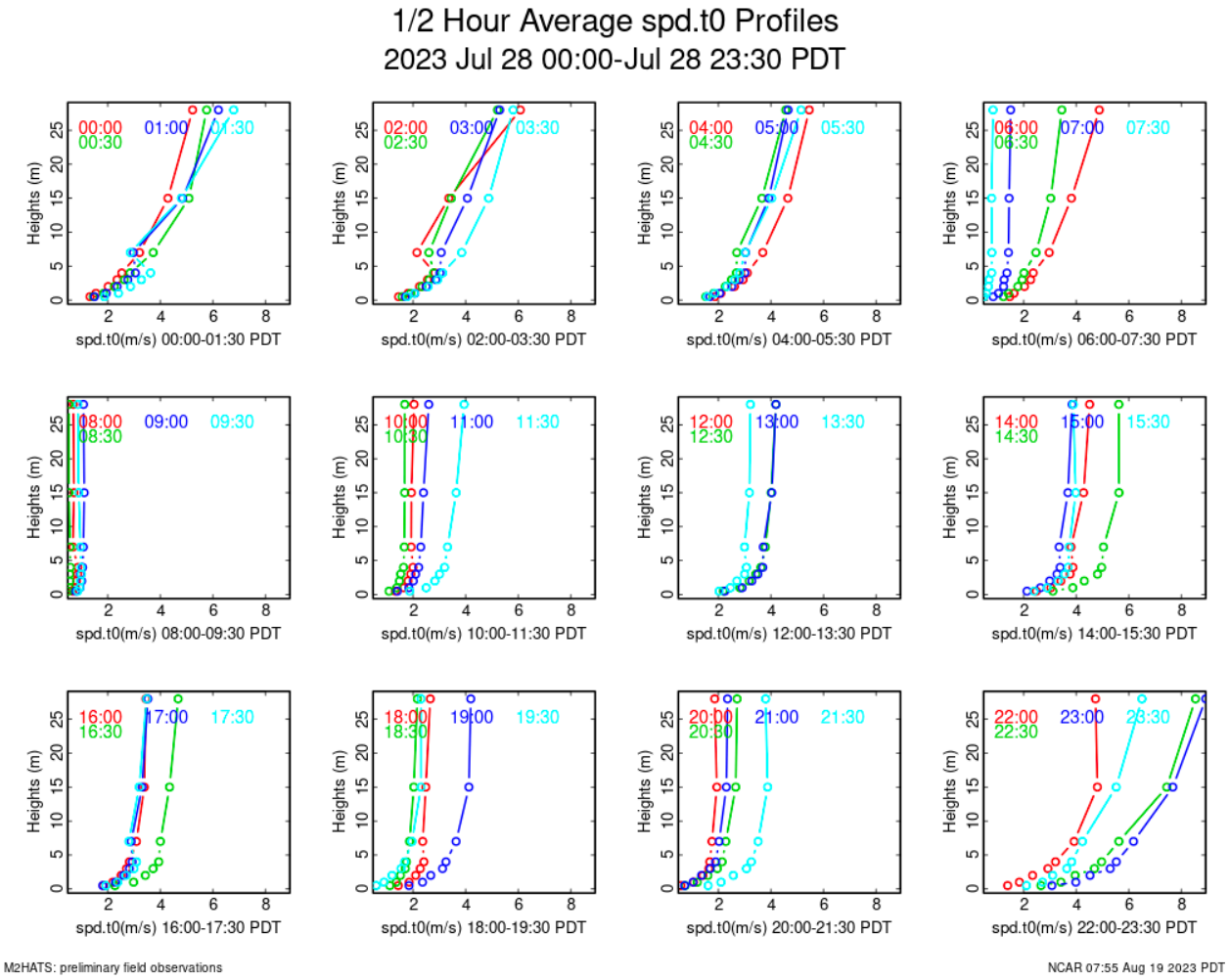


Figure 6. Profiles of 30 min averaged wind speeds at the t0 tower. There is a kink at the 0200 - 0300 PDT profiles that has been slightly mitigated by extending the 7m boom from 5m to 10m on 31 July. These preliminary plots can be accessed for the entire project period at https://archive.eol.ucar.edu/docs/isf/projects/M2HATS/isfs/qcdata/

Theodolite Geographic Coordinates and Tilt Corrections

As part of the total survey of M2HATS anemometer instrumentation, the Leica Multistation (MS60 laser theodolite) made scans of the positions and orientation of each sonic anemometer with respect to gravity. The scans were georeferenced using a stand-alone GPS receiver. Refer to wind direction quick reference guide on converting Campbell CSAT3 sonics between instrument and geographic coordinates

The Leica theodolite measures distances relative to itself using a very precise laser and knowledge of its azimuth, with respect to true north, and elevation angle. The distances are measured in x, y coordinates, using the Universal Transverse Mercator (UTM) geodetic projection, and converted to true headings. The GRS 1980 ellipsoid was the reference surface used for the positions.

The flux towers masts/tripods were constructed to face roughly parallel to the local height contours and the anemometer boom to be mounted on this face, i.e. wind from the un-obstructed direction. This was done to minimize distortion of the flow by the mast for winds perpendicular to the ridge lines and also capture up and down valley flows. Although local surrounding obstacles (ridges, trees, shrubs, poles, gates) may interfere with the anemometer.

In order to report winds in geographic coordinates, the orientation of the instrument needs to be known to rotate the wind vectors into geographic coordinates. With a measured azimuth angle taken along the boom mounted sonics, the orientation is known since every anemometer head is rigidly attached to the boom and the sonic heads are attached in a captive manner.

The tilt of a sonic anemometer from true vertical can introduce errors in the measured sensible heat and momentum fluxes. The tilt error in a scalar flux is on the order of 5% per degree of tilt in the vertical plane aligned with the mean wind direction (Steve Oncley, personal communication). Consequently, it is often necessary to rotate the coordinates of three-dimensional sonic wind data to correct for this tilt.

We shoot the center of the anemometer sphere at the top and bottom of the CSAT3 transducers, to which we add the sphere's radius to obtain the exact x, y, z position of these spheres. We also shoot the mounting boom near the sonic and near the tower, and add the radius of the boom. From these coordinates, we can calculate the pitch and roll angles (and azimuth) of the sonic array. We input this information into our "calibration files" as lean and lean azimuth, using the formulae:

```
deg2rad = pi/180
b3 = tan(-roll*deg2rad)
```

```
b2 = tan(pitch*deg2rad)/cos(roll*deg2rad)
lean = round(atan(sqrt(b2^2 + b3^2))/deg2rad, 1)
leanaz = round(atan2(-b3, -b2)/deg2rad, 1)
```

Azimuth measurements

Azimuth, pitch and roll calculated by the Leica laser scanning theodolite for each anemometer are provided in **Table 6.** We use the Azimuth to adjust the wind vectors where the +V axis points north. Sonics are adjusted relative to gravity using the azimuth, pitch, and roll measured by the Leica.

The Leica boom coordinates for T25 were incorrect; therefore, a wind field comparison with T24 and T26 was used to best estimate the boom angle of T25 and the pitch and roll of T25 were set to the default of 0 degrees. Additionally one Leica coordinate for the T35 sonic was incorrect. The T35 boom coordinates were correct, so the Azimuth and Pitch could be correctly calculated, but the Roll could not be calculated and had to be set to the default of 0 degrees.

Table 6. Azimuth angles and orientation as measured by the Leica for each anemometer at the beginning of the project (end of July). Leica scans aimed between the vertical tower pole and centerline of the boom on which the anemometer is mounted.

Site	Azimuth (deg)	Pitch (deg)	Roll (deg)
t0p	261.87	-0.563	0.00
t01	262.15	-1.331	-1.253
t02	260.63	-1.165	-1.563
t03	257.48	-1.095	-1.266
t04	260.34	-0.399	-0.530
t05	261.25	-1.547	-1.423
t06	258.53	0.128	-0.868
t07	260.29	-0.922	-0.481
t08	258.98	-0.883	-0.571
t09	261.16	-0.377	-0.168
t10	258.11	-1.166	-1.785

t11	258.16	-2.041	-2.175
t12	260.22	-0.731	-0.885
t13	260.19	-1.046	-2.030
t14	259.59	-1.190	-3.196
t15	259.78	-0.378	-1.768
t16	259.93	-1.204	-2.511
t17	263.24	-1.133	-2.295
t18	259.97	-0.410	-2.066
t19	258.5	-0.491	-2.939
t20	262.45	-0.714	-1.552
t21	261.4	-1.008	-1.248
t22	258.35	-1.101	-2.797
t23	260.94	-1.238	-2.963
t24	257.19	-0.816	-2.154
t25	256.44	0.000	0.000
t26	257.83	-0.713	-2.149
t27	261.16	-0.515	-2.473
t28	264.31	-1.346	-1.998
t29	257.49	-1.288	-2.470
t30	261.92	0.167	1.434
t31	260.75	-0.195	0.095
t32	255.85	-1.500	-1.717
t33	261.59	-0.889	-0.457
t34	261.12	-1.488	-2.355
t35	259.85	-1.347	0.000
t36	256.46	-1.197	-0.139

t37	262.23	-0.228	0.230
t38	263.4	-2.319	-2.841
t39	261.09	-0.937	-1.138
t40	257.74	-1.165	-0.238
t41	259.26	-1.335	-0.426
t42	259.82	-1.0479	-1.170
t43	261.22	-0.721	0.123
t44	260.23	-0.645	-0.030
t45	259.99	-1.050	-1.432
t46	258.91	-1.309	0.066
t47	258.62	-1.232	1.600
t48	257.11	-1.487	0.455
t49	259.55	-0.896	0.236
t0_0.5	260.47	-1.264	-1.653
t0_1	260.06	-1.687	-1.613
t0_2	259.81	-1.289	-1.734
t0_3	259.56	-0.983	-1.765
t0_4	259.11	-1.618	-1.921
t0_7	259.39	-1.339	0.782
t0_15	259.61	-0.591	1.429
t0_28	259.29	-1.195	1.258

Sonic Calibrations

Sonic anemometers performed calibration checks in an environmental chamber that operated over a defined stated temperature range (-30°C to +50°C). The anemometers were calibrated with three orientations (on the x, y, z axes) and the u component was examined. Overall, the u component measured deviations between 0.0 cm/s and 0.3 cm/s with a standard deviation of +/- 0.1 cm/s. All sonics performed within specification and no adjustments were made.

The diagnostic variable ldiag is the sonic anemometer flag. The most common cause of non-zero diagbits is the presence of water droplets on the anemometer transducers. Sonic values should be set to nan's if any of the bits are non-zero. For averaged values - ldiag is an average of a logical diagnostic over the period, with a value of 0 or 1 indicating whether diagbits was non-zero. The average of ldiag is then the fraction of samples over each average period that diagbits was non-zero. To screen averaged data, choose a maximum allowed value for ldiag, for example 0.01 or 0.02, and discard the means or covariances for a sonic when ldiag exceeds that value.

EC150 Infrared Gas Analyzer (H_2O/CO_2)

The CSAT3A was coupled with an infrared absorption gas analyzer (EC-150 IRGA) to measure H_2O and CO_2.

The sensors were filtered for

- irgadiag not equal to 0
- Negative spikes in H_2O that are not captured by the internal diagnostics.
- Minimum and Maximum values of 0 and 100 g/m^3 for H_2O and a cap of 10 g/m^3 for CO_2 to remove any outliers.

EC150 variables should be set to the not-a-number fill value for when irgadiag is non-zero. We have noticed this does not happen in all cases. We recommend the user re-apply the `irgadiag` $\neq 0$ filtering criteria when using these data. `irgadiag` also refers to excessive moisture affecting sensor operations.

EC150 variables also have an associated SS (signal strength variable). Low SS values are associated with rain events seen in the disdrometer ‘rainr’ rain rate variable and increasing in RH data. See Rain Events **Table 5** and **Figure 6.** Note that the signal strength is unique to each sensor. We recommend caution when using H_2O and CO_2 measurements when SS values drop.

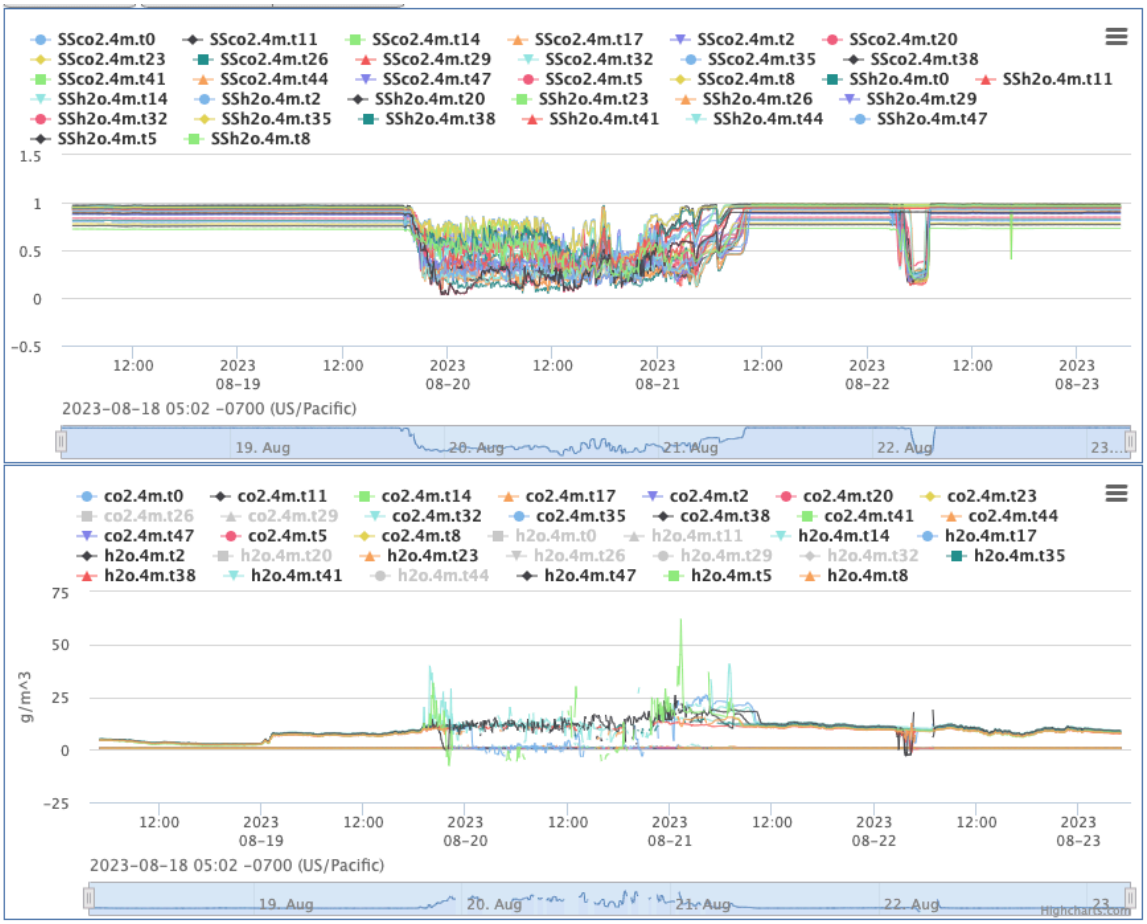


Figure 6 The SS (signal strength) of the H_2O and CO_2 data across many of the towers at the 4 meter level is plotted for the 2023-08-18 05:00 PDT to 2023-08-23 05:00 PDT time range in the top plot. The H_2O and CO_2 data across many of the towers at the 4 meter level is plotted for the 2023-08-18 05:00 PDT to 2023-08-23 05:00 PDT. The largest rain event during the M2HATS operations, Storm Hilary, occurred 2023-08-19 19:00 PDT to 2023-08-21 11:00 PDT when the SS values decreased and the various H_2O and CO_2 produced noisy values.

H_2O

H_2O sensors operated as expected and measurements showed no significant biases during the project (**Figure 7**).

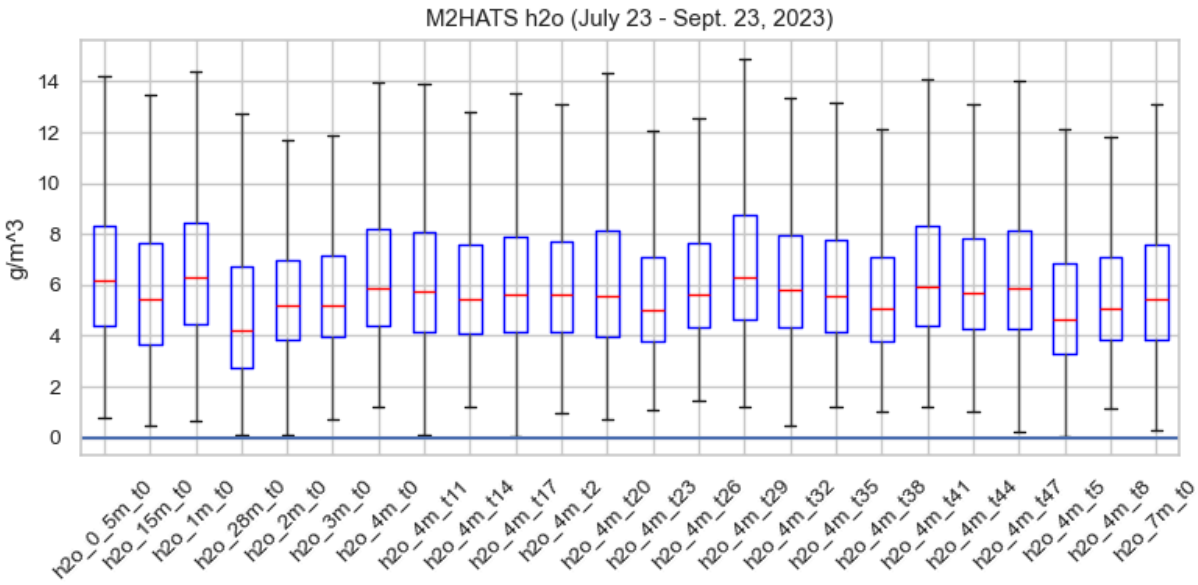


Figure 7. Box and whisker plots H_2O for the entire period of the project for all operating gas analyzers.

CO_2

The co2.28m.t0 sensor unfortunately was not working properly for many days. The values were uncharacteristically high, and they were associated with a prominent diurnal cycle. These data were removed from 2023-07-22 until 2023-09-04 13:00 PDT when the sensor was replaced at 28 meters on the t0 tower.

From **Figure 8** significant low biases in co2 were observed in co2_1m_t0, co2_4m_t0, co2_4m_t20, co2_4m_t47. We adjust the measurement based on the mean of all other samples which was calculated to be 0.6224 g/m^3. We made the following upward adjustments to the fours variables:

co2_1m_t0 - added +0.168 g/m^3
co2_4m_t0 - added +0.110 g/m^3
co2_4m_t20 - added +0.098 g/m^3
co2_4m_t47 - added +0.086 g/m^3

In **Figure 8**, you can see the results of adding the adjusted amounts to the four CO_2 time series on the far right side of the plot.

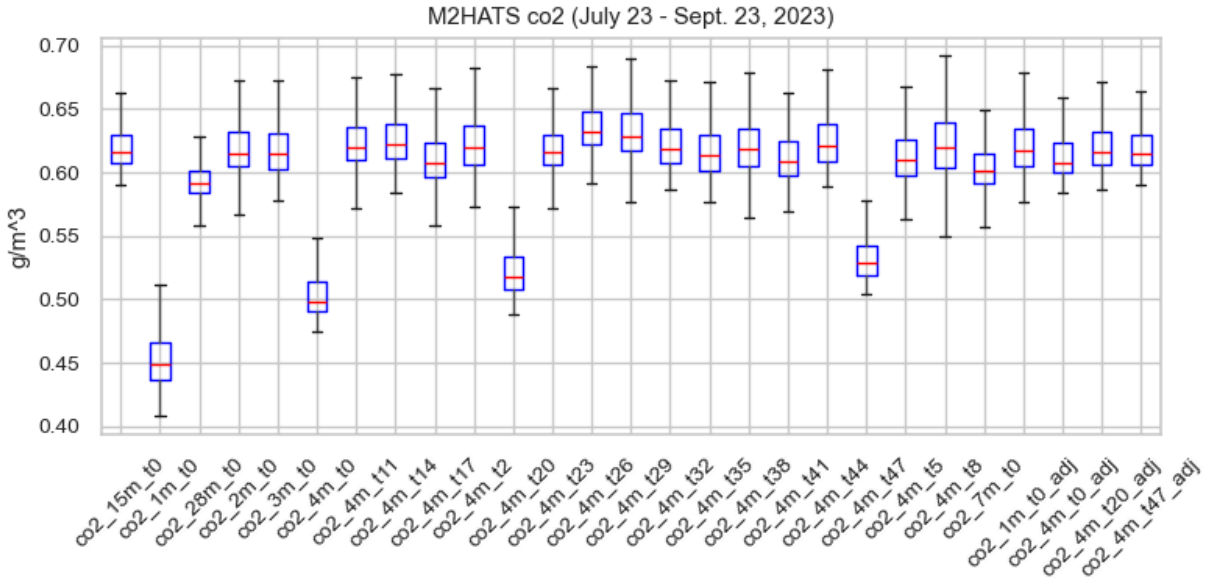


Figure 8. Box and whisker plots CO_2 for the entire period of the project for all operating gas analyzers. The last four variables plotted on the right hand side are the final adjusted values to co2_1m_t0, co2_4m_t0, co2_4m_t20, and co2_4m_t47 which fall within the range of the rest of the CO_2 sensor measurements.

Soils

All soil sensors (NCAR 4-level Tsoil, Meter EC-5 Qsoil, REBS HFT Gsoil, and Hukseflux TP01 thermal properties) were buried at 0 – 5 cm layer at sites t2, t23, and t49 - to span the center and edges of the horizontal array. Refer to documentation on the installation of soil sensors for more details.

Heat flux, Gsoil

No issues noted during operations. No problems were found during QC processing. Calculations of the heat flux at the surface, corrected for the Phillip correction and heat storage within the 0--5 cm layer of soil using the Tsoil and TP01 data and as described in calculation of soil heat flux at the surface have been added to the 5-minute NetCDF files.

Soil Temperature, Tsoil

Calibrations of the Tsoils were performed in the EOL Calibration Laboratory : https://www.eol.ucar.edu/research-development/calibration-laboratory/calibration-laboratory-resources. Temperature oil baths were used to calibrate the Tsoils, similar to the temperature probes of the TRH's. A few spikes were identified and filtered. Otherwise, no issues were noted during operations.

Soil Moisture, Qsoil

The soil moisture sensor (Qsoil) was installed at a depth of 2.5 cm. We used the manufacturer's calibration values for potting soil.

Four soil samples were taken during the course of the field project. These samples were used to measure soil moisture content by the gravimetric method: a fresh soil core sample is weighed, oven dried until there is no further mass loss, and then reweighed. The moisture content is expressed as mass of water per mass of dry soil. **Figure 9** are the comparisons between Qsoil and the gravimetric results.

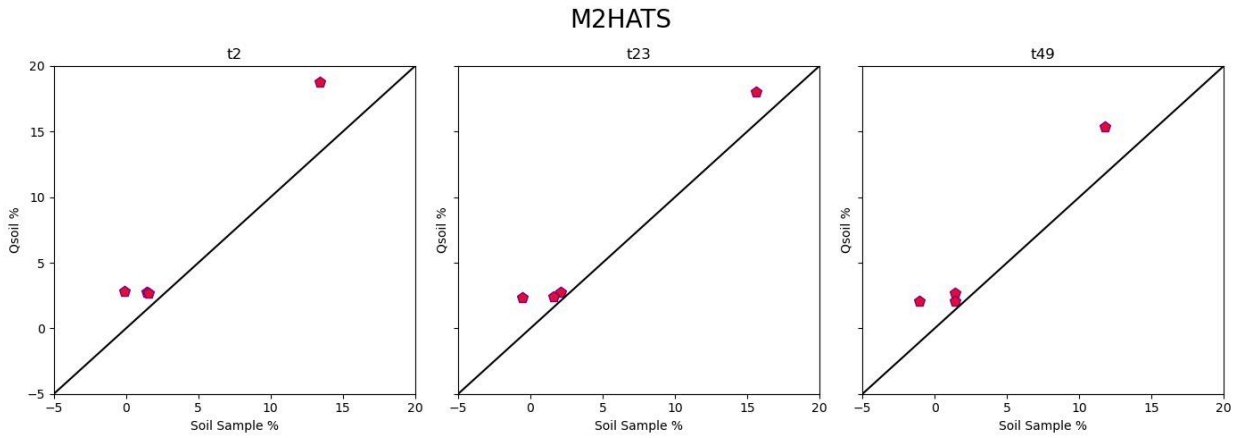


Figure 9. Comparison of Qsoil to the gravimetric soil moisture for each site.

The gravimetric samples also produce values for the bulk density of the soil at each site. These values are shown in **Table 7**.

Table 7. Bulk density, in g/cm^3, of the soil at each site.

Site	Sample 1	Sample 2	Sample 3	Sample 4
t2	1.41	1.42	1.52	1.09
t23	1.41	1.31	1.38	1.02
t49	1.58	1.61	1.51	1.07

Soil thermal properties (TP01)

The Hukseflux TP01 sends a heat pulse into the soil every 3 hours and measures the resulting change in temperature. From these measurements of heating (Vheat), thermopile response (Vpile), and the temperature delay time constant (Tau63), and the thermal conductivity (Lambda) can be calculated.

Data notes:

The Lambda and Tau63 measurements at site t23 started to deviate from those at the t2 and t49 sites. This deviation coincides with the Storm Hilary event starting around 2023-08-21 00:00 PDT. There were some issues noted with water in the cooler at t23, but the t23 TP01 sensors never realign with the t2 and t39 sensors. Thus, data has been removed for the time period starting on 2023-08-21 for Lambda.t23 and Tau63.t23 for the remainder of operations.

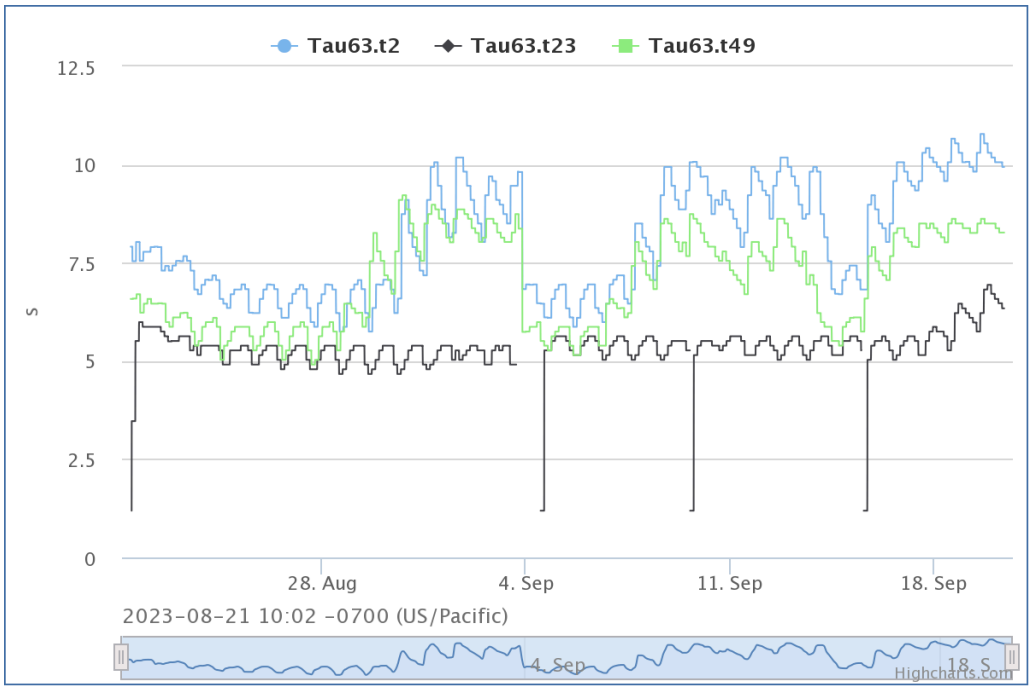


Figure 10. Time series of preliminary Tau63.t2, Tau63.t23, and Tau63.t49 after Storm Hilary demonstrating Tau63.t23 not aligning with the corresponding TP01 soil sensor values.

Percival2 Ott Disdrometer

No issues noted during operations.

Data Availability

Figure 11 shows the overall percent of 5-minute ISFS sensor data remaining per variable, at all heights, after all quality checks and filters have been applied. The lower data capture of sonic data at t0p was due to a late set-up (July 27th). Thermal conductivity (Lambda) and decay time (Tau63) at site t23 are low because of a bad TP01 sensor after storm Hilary.

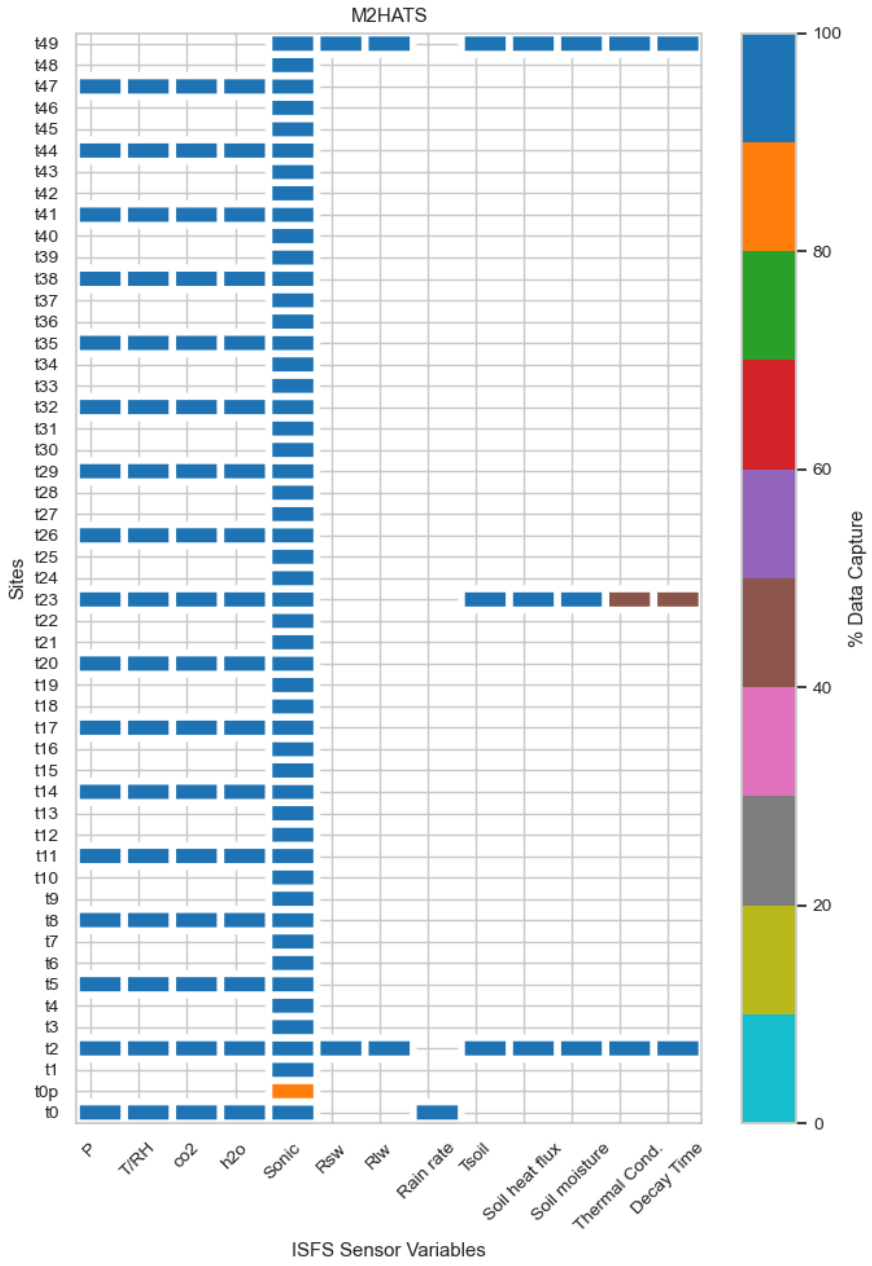


Figure 11. Percent of data available during M2HATS. Most major ISFS sensor datasets are included. Blank areas (or NaN's) denote no sensors were operating.

Minor Data Gaps

Small data gaps occur from time to time in a given sensors' data stream. These may be due to

- Loss of GPS signal when rebooting due to loss of power due to maintenance, i.e. servicing sensors.
- Sensor thresholds on the data.
- Status or error messages from the sensor.

Appendix A

CSAT model used at each array tower.

Site	3D CSAT sonic and IRGA EC150 configuration
t0p	CSAT3A
t1	CSAT3 until Aug. 8 13:00, switched to CSAT3A thereafter
t2	CSAT3A + EC150
t3	CSAT3
t4	CSAT3
t5	CSAT3A + EC150
t6	CSAT3B
t7	CSAT3
t8	CSAT3A + EC150
t9	CSAT3A
t10	CSAT3
t11	CSAT3A + EC150
t12	CSAT3B
t13	CSAT3
t14	CSAT3A + EC150
t15	CSAT3A
t16	CSAT3
t17	CSAT3A + EC150
t18	CSAT3B
t19	CSAT3
t20	CSAT3A + EC150
t21	CSAT3A
t22	CSAT3

t23	CSAT3A + EC150
t24	CSAT3B
t25	CSAT3
t26	CSAT3A + EC150
t27	CSAT3A
t28	CSAT3
t29	CSAT3A + EC150
t30	CSAT3B
t31	CSAT3
t32	CSAT3A + EC150
t33	CSAT3
t34	CSAT3
t35	CSAT3A + EC150
t36	CSAT3B
t37	CSAT3
t38	CSAT3A + EC150
t39	CSAT3
t40	CSAT3
t41	CSAT3A + EC150
t42	CSAT3B
t43	CSAT3
t44	CSAT3A + EC150
t45	CSAT3
t46	CSAT3
t47	CSAT3A + EC150
t48	CSAT3B
t49	CSAT3

Appendix B

A snapshot of the list of all variables in the high rate dataset. Note that it does not take into account configuration changes when sensors were replaced during operations. Please use this table merely as a dictionary of variable naming conventions and definitions..

Variable Name	Samples/s	Sensor	Short Description
u.1m.t0	60	CSAT3_IRGA_BIN	Wind U component, CSAT3
v.1m.t0	60	CSAT3_IRGA_BIN	Wind V component, CSAT3
w.1m.t0	60	CSAT3_IRGA_BIN	Wind W component, CSAT3
tc.1m.t0	60	CSAT3_IRGA_BIN	Virtual air temperature from speed of sound, CSAT3
diagbits.1m.t0	60	CSAT3_IRGA_BIN	CSAT3 diagnostic sum, 1=low sig,2=high sig,4=no lock,8=path diff,16=skipped samp
co2.1m.t0	60	CSAT3_IRGA_BIN	CO_2 density from CSI IRGA
h2o.1m.t0	60	CSAT3_IRGA_BIN	Water vapor density from CSI IRGA
irgadiag.1m.t0	60	CSAT3_IRGA_BIN	CSI IRGA diagnostic
Tirga.1m.t0	60	CSAT3_IRGA_BIN	CSI IRGA temperature
Pirga.1m.t0	60	CSAT3_IRGA_BIN	CSI IRGA pressure
ldiag.1m.t0	60	CSAT3_IRGA_BIN	CSAT3 logical diagnostic, 0=OK, 1=(diagbits!=0)
T.1m.t0	1	NCAR_SHT	Air Temperature, NCAR hygro-thermometer
RH.1m.t0	1	NCAR_SHT	Relative Humidity, NCAR hygro-thermometer
P.1m.t0	20	Nano	Barometric Pressure, Paroscientific 6000
u.2m.t0	60	CSAT3_IRGA_BIN	Wind U component, CSAT3
v.2m.t0	60	CSAT3_IRGA_BIN	Wind V component, CSAT3
w.2m.t0	60	CSAT3_IRGA_BIN	Wind W component, CSAT3
tc.2m.t0	60	CSAT3_IRGA_BIN	Virtual air temperature from speed of sound, CSAT3
diagbits.2m.t0	60	CSAT3_IRGA_BIN	CSAT3 diagnostic sum, 1=low sig,2=high sig,4=no lock,8=path diff,16=skipped samp
co2.2m.t0	60	CSAT3_IRGA_BIN	CO_2 density from CSI IRGA
h2o.2m.t0	60	CSAT3_IRGA_BIN	Water vapor density from CSI IRGA
irgadiag.2m.t0	60	CSAT3_IRGA_BIN	CSI IRGA diagnostic
Tirga.2m.t0	60	CSAT3_IRGA_BIN	CSI IRGA temperature
Pirga.2m.t0	60	CSAT3_IRGA_BIN	CSI IRGA pressure
ldiag.2m.t0	60	CSAT3_IRGA_BIN	CSAT3 logical diagnostic, 0=OK, 1=(diagbits!=0)
P.2m.t0	20	Nano	Barometric Pressure, Paroscientific 6000
u.0.5m.t0	60	CSAT3_IRGA_BIN	Wind U component, CSAT3
v.0.5m.t0	60	CSAT3_IRGA_BIN	Wind V component, CSAT3
w.0.5m.t0	60	CSAT3_IRGA_BIN	Wind W component, CSAT3
tc.0.5m.t0	60	CSAT3_IRGA_BIN	Virtual air temperature from speed of sound, CSAT3

diagbits.0.5m.t0	60	CSAT3_IRGA_BIN	CSAT3 diagnostic sum, 1=low sig,2=high sig,4=no lock,8=path diff,16=skipped samp
co2.0.5m.t0	60	CSAT3_IRGA_BIN	CO_2 density from CSI IRGA
h2o.0.5m.t0	60	CSAT3_IRGA_BIN	Water vapor density from CSI IRGA
irgadiag.0.5m.t0	60	CSAT3_IRGA_BIN	CSI IRGA diagnostic
Tirga.0.5m.t0	60	CSAT3_IRGA_BIN	CSI IRGA temperature
Pirga.0.5m.t0	60	CSAT3_IRGA_BIN	CSI IRGA pressure
ldiag.0.5m.t0	60	CSAT3_IRGA_BIN	CSAT3 logical diagnostic, 0=OK, 1=(diagbits!=0)
P.0.5m.t0	20	Nano	Barometric Pressure, Paroscientific 6000
u.3m.t0	60	CSAT3_IRGA_BIN	Wind U component, CSAT3
v.3m.t0	60	CSAT3_IRGA_BIN	Wind V component, CSAT3
w.3m.t0	60	CSAT3_IRGA_BIN	Wind W component, CSAT3
tc.3m.t0	60	CSAT3_IRGA_BIN	Virtual air temperature from speed of sound, CSAT3
diagbits.3m.t0	60	CSAT3_IRGA_BIN	CSAT3 diagnostic sum, 1=low sig,2=high sig,4=no lock,8=path diff,16=skipped samp
co2.3m.t0	60	CSAT3_IRGA_BIN	CO_2 density from CSI IRGA
h2o.3m.t0	60	CSAT3_IRGA_BIN	Water vapor density from CSI IRGA
irgadiag.3m.t0	60	CSAT3_IRGA_BIN	CSI IRGA diagnostic
Tirga.3m.t0	60	CSAT3_IRGA_BIN	CSI IRGA temperature
Pirga.3m.t0	60	CSAT3_IRGA_BIN	CSI IRGA pressure
ldiag.3m.t0	60	CSAT3_IRGA_BIN	CSAT3 logical diagnostic, 0=OK, 1=(diagbits!=0)
T.3m.t0	1	NCAR_SHT	Air Temperature, NCAR hygro-thermometer
RH.3m.t0	1	NCAR_SHT	Relative Humidity, NCAR hygro-thermometer
P.3m.t0	20	Nano	Barometric Pressure, Paroscientific 6000
u.4m.t0	60	CSAT3_IRGA_BIN	Wind U component, CSAT3
v.4m.t0	60	CSAT3_IRGA_BIN	Wind V component, CSAT3
w.4m.t0	60	CSAT3_IRGA_BIN	Wind W component, CSAT3
tc.4m.t0	60	CSAT3_IRGA_BIN	Virtual air temperature from speed of sound, CSAT3
diagbits.4m.t0	60	CSAT3_IRGA_BIN	CSAT3 diagnostic sum, 1=low sig,2=high sig,4=no lock,8=path diff,16=skipped samp
co2.4m.t0	60	CSAT3_IRGA_BIN	CO_2 density from CSI IRGA
h2o.4m.t0	60	CSAT3_IRGA_BIN	Water vapor density from CSI IRGA
irgadiag.4m.t0	60	CSAT3_IRGA_BIN	CSI IRGA diagnostic
Tirga.4m.t0	60	CSAT3_IRGA_BIN	CSI IRGA temperature
Pirga.4m.t0	60	CSAT3_IRGA_BIN	CSI IRGA pressure
ldiag.4m.t0	60	CSAT3_IRGA_BIN	CSAT3 logical diagnostic, 0=OK, 1=(diagbits!=0)
T.4m.t0	1	NCAR_SHT	Air Temperature, NCAR hygro-thermometer
RH.4m.t0	1	NCAR_SHT	Relative Humidity, NCAR hygro-thermometer

P.4m.t0	20	Nano	Barometric Pressure, Paroscientific 6000
T.0.5m.t0	1	NCAR_SHT	Air Temperature, NCAR hygro-thermometer
RH.0.5m.t0	1	NCAR_SHT	Relative Humidity, NCAR hygro-thermometer
T.2m.t0	1	NCAR_SHT	Air Temperature, NCAR hygro-thermometer
RH.2m.t0	1	NCAR_SHT	Relative Humidity, NCAR hygro-thermometer
u.7m.t0	60	CSAT3_IRGA_BIN	Wind U component, CSAT3
v.7m.t0	60	CSAT3_IRGA_BIN	Wind V component, CSAT3
w.7m.t0	60	CSAT3_IRGA_BIN	Wind W component, CSAT3
tc.7m.t0	60	CSAT3_IRGA_BIN	Virtual air temperature from speed of sound, CSAT3
diagbits.7m.t0	60	CSAT3_IRGA_BIN	CSAT3 diagnostic sum, 1=low sig,2=high sig,4=no lock,8=path diff,16=skipped samp
co2.7m.t0	60	CSAT3_IRGA_BIN	CO_2 density from CSI IRGA
h2o.7m.t0	60	CSAT3_IRGA_BIN	Water vapor density from CSI IRGA
irgadiag.7m.t0	60	CSAT3_IRGA_BIN	CSI IRGA diagnostic
Tirga.7m.t0	60	CSAT3_IRGA_BIN	CSI IRGA temperature
Pirga.7m.t0	60	CSAT3_IRGA_BIN	CSI IRGA pressure
ldiag.7m.t0	60	CSAT3_IRGA_BIN	CSAT3 logical diagnostic, 0=OK, 1=(diagbits!=0)
T.7m.t0	1	NCAR_SHT	Air Temperature, NCAR hygro-thermometer
RH.7m.t0	1	NCAR_SHT	Relative Humidity, NCAR hygro-thermometer
P.7m.t0	20	Nano	Barometric Pressure, Paroscientific 6000
u.15m.t0	60	CSAT3_IRGA_BIN	Wind U component, CSAT3
v.15m.t0	60	CSAT3_IRGA_BIN	Wind V component, CSAT3
w.15m.t0	60	CSAT3_IRGA_BIN	Wind W component, CSAT3
tc.15m.t0	60	CSAT3_IRGA_BIN	Virtual air temperature from speed of sound, CSAT3
diagbits.15m.t0	60	CSAT3_IRGA_BIN	CSAT3 diagnostic sum, 1=low sig,2=high sig,4=no lock,8=path diff,16=skipped samp
co2.15m.t0	60	CSAT3_IRGA_BIN	CO_2 density from CSI IRGA
h2o.15m.t0	60	CSAT3_IRGA_BIN	Water vapor density from CSI IRGA
irgadiag.15m.t0	60	CSAT3_IRGA_BIN	CSI IRGA diagnostic
Tirga.15m.t0	60	CSAT3_IRGA_BIN	CSI IRGA temperature
Pirga.15m.t0	60	CSAT3_IRGA_BIN	CSI IRGA pressure
ldiag.15m.t0	60	CSAT3_IRGA_BIN	CSAT3 logical diagnostic, 0=OK, 1=(diagbits!=0)
T.15m.t0	1	NCAR_SHT	Air Temperature, NCAR hygro-thermometer
RH.15m.t0	1	NCAR_SHT	Relative Humidity, NCAR hygro-thermometer
P.15m.t0	20	Nano	Barometric Pressure, Paroscientific 6000
u.28m.t0	60	CSAT3_IRGA_BIN	Wind U component, CSAT3
v.28m.t0	60	CSAT3_IRGA_BIN	Wind V component, CSAT3

w.28m.t0	60	CSAT3_IRGA_BIN	Wind W component, CSAT3
tc.28m.t0	60	CSAT3_IRGA_BIN	Virtual air temperature from speed of sound, CSAT3
diagbits.28m.t0	60	CSAT3_IRGA_BIN	CSAT3 diagnostic sum, 1=low sig,2=high sig,4=no lock,8=path diff,16=skipped samp
co2.28m.t0	60	CSAT3_IRGA_BIN	CO_2 density from CSI IRGA
h2o.28m.t0	60	CSAT3_IRGA_BIN	Water vapor density from CSI IRGA
irgadiag.28m.t0	60	CSAT3_IRGA_BIN	CSI IRGA diagnostic
Tirga.28m.t0	60	CSAT3_IRGA_BIN	CSI IRGA temperature
Pirga.28m.t0	60	CSAT3_IRGA_BIN	CSI IRGA pressure
ldiag.28m.t0	60	CSAT3_IRGA_BIN	CSAT3 logical diagnostic, 0=OK, 1=(diagbits!=0)
T.28m.t0	1	NCAR_SHT	Air Temperature, NCAR hygro-thermometer
RH.28m.t0	1	NCAR_SHT	Relative Humidity, NCAR hygro-thermometer
P.28m.t0	20	Nano	Barometric Pressure, Paroscientific 6000
u.4m.t1	30	CSAT3	Wind U component, CSAT3
v.4m.t1	30	CSAT3	Wind V component, CSAT3
w.4m.t1	30	CSAT3	Wind W component, CSAT3
tc.4m.t1	30	CSAT3	Virtual air temperature from speed of sound, CSAT3
diagbits.4m.t1	30	CSAT3	CSAT3 diagnostic sum, 1=low sig,2=high sig,4=no lock,8=path diff,16=skipped samp
ldiag.4m.t1	30	CSAT3	CSAT3 logical diagnostic, 0=OK, 1=(diagbits!=0)
u.4m.t2	60	CSAT3_IRGA_BIN	Wind U component, CSAT3
v.4m.t2	60	CSAT3_IRGA_BIN	Wind V component, CSAT3
w.4m.t2	60	CSAT3_IRGA_BIN	Wind W component, CSAT3
tc.4m.t2	60	CSAT3_IRGA_BIN	Virtual air temperature from speed of sound, CSAT3
diagbits.4m.t2	60	CSAT3_IRGA_BIN	CSAT3 diagnostic sum, 1=low sig,2=high sig,4=no lock,8=path diff,16=skipped samp
co2.4m.t2	60	CSAT3_IRGA_BIN	CO_2 density from CSI IRGA
h2o.4m.t2	60	CSAT3_IRGA_BIN	Water vapor density from CSI IRGA
irgadiag.4m.t2	60	CSAT3_IRGA_BIN	CSI IRGA diagnostic
Tirga.4m.t2	60	CSAT3_IRGA_BIN	CSI IRGA temperature
Pirga.4m.t2	60	CSAT3_IRGA_BIN	CSI IRGA pressure
ldiag.4m.t2	60	CSAT3_IRGA_BIN	CSAT3 logical diagnostic, 0=OK, 1=(diagbits!=0)
T.4m.t2	1	NCAR_SHT	Air Temperature, NCAR hygro-thermometer
RH.4m.t2	1	NCAR_SHT	Relative Humidity, NCAR hygro-thermometer
P.4m.t2	20	Nano	Barometric Pressure, Paroscientific 6000
u.4m.t3	30	CSAT3	Wind U component, CSAT3
v.4m.t3	30	CSAT3	Wind V component, CSAT3
w.4m.t3	30	CSAT3	Wind W component, CSAT3

tc.4m.t3	30	CSAT3	Virtual air temperature from speed of sound, CSAT3
diagbits.4m.t3	30	CSAT3	CSAT3 diagnostic sum, 1=low sig,2=high sig,4=no lock,8=path diff,16=skipped samp
ldiag.4m.t3	30	CSAT3	CSAT3 logical diagnostic, 0=OK, 1=(diagbits!=0)
u.4m.t0p	60	CSAT3A_BIN	Wind U component, CSAT3
v.4m.t0p	60	CSAT3A_BIN	Wind V component, CSAT3
w.4m.t0p	60	CSAT3A_BIN	Wind W component, CSAT3
tc.4m.t0p	60	CSAT3A_BIN	Virtual air temperature from speed of sound, CSAT3
diagbits.4m.t0p	60	CSAT3A_BIN	CSAT3 diagnostic sum, 1=low sig,2=high sig,4=no lock,8=path diff,16=skipped samp
ldiag.4m.t0p	60	CSAT3A_BIN	CSAT3 logical diagnostic, 0=OK, 1=(diagbits!=0)
u.4m.t4	30	CSAT3	Wind U component, CSAT3
v.4m.t4	30	CSAT3	Wind V component, CSAT3
w.4m.t4	30	CSAT3	Wind W component, CSAT3
tc.4m.t4	30	CSAT3	Virtual air temperature from speed of sound, CSAT3
diagbits.4m.t4	30	CSAT3	CSAT3 diagnostic sum, 1=low sig,2=high sig,4=no lock,8=path diff,16=skipped samp
ldiag.4m.t4	30	CSAT3	CSAT3 logical diagnostic, 0=OK, 1=(diagbits!=0)
u.4m.t5	60	CSAT3_IRGA_BIN	Wind U component, CSAT3
v.4m.t5	60	CSAT3_IRGA_BIN	Wind V component, CSAT3
w.4m.t5	60	CSAT3_IRGA_BIN	Wind W component, CSAT3
tc.4m.t5	60	CSAT3_IRGA_BIN	Virtual air temperature from speed of sound, CSAT3
diagbits.4m.t5	60	CSAT3_IRGA_BIN	CSAT3 diagnostic sum, 1=low sig,2=high sig,4=no lock,8=path diff,16=skipped samp
co2.4m.t5	60	CSAT3_IRGA_BIN	CO_2 density from CSI IRGA
h2o.4m.t5	60	CSAT3_IRGA_BIN	Water vapor density from CSI IRGA
irgadiag.4m.t5	60	CSAT3_IRGA_BIN	CSI IRGA diagnostic
Tirga.4m.t5	60	CSAT3_IRGA_BIN	CSI IRGA temperature
Pirga.4m.t5	60	CSAT3_IRGA_BIN	CSI IRGA pressure
ldiag.4m.t5	60	CSAT3_IRGA_BIN	CSAT3 logical diagnostic, 0=OK, 1=(diagbits!=0)
T.4m.t5	1	NCAR_SHT	Air Temperature, NCAR hygro-thermometer
RH.4m.t5	1	NCAR_SHT	Relative Humidity, NCAR hygro-thermometer
P.4m.t5	20	Nano	Barometric Pressure, Paroscientific 6000
u.4m.t6	50	CSAT3B	Wind U component, CSAT3BH
v.4m.t6	50	CSAT3B	Wind V component, CSAT3BH
w.4m.t6	50	CSAT3B	Wind W component, CSAT3BH
tc.4m.t6	50	CSAT3B	Virtual air temperature from speed of sound, CSAT3BH
diag.4m.t6	50	CSAT3B	CSAT3BH diagnostic sum

ldiag.4m.t6	50	CSAT3B	CSAT3BH logical diagnostic, 0=OK, 1=(diagbits!=0)
u.4m.t7	50	CSAT3B	Wind U component, CSAT3BH
v.4m.t7	50	CSAT3B	Wind V component, CSAT3BH
w.4m.t7	50	CSAT3B	Wind W component, CSAT3BH
tc.4m.t7	50	CSAT3B	Virtual air temperature from speed of sound, CSAT3BH
diag.4m.t7	50	CSAT3B	CSAT3BH diagnostic sum
ldiag.4m.t7	50	CSAT3B	CSAT3BH logical diagnostic, 0=OK, 1=(diagbits!=0)
u.4m.t8	60	CSAT3_IRGA_BIN	Wind U component, CSAT3
v.4m.t8	60	CSAT3_IRGA_BIN	Wind V component, CSAT3
w.4m.t8	60	CSAT3_IRGA_BIN	Wind W component, CSAT3
tc.4m.t8	60	CSAT3_IRGA_BIN	Virtual air temperature from speed of sound, CSAT3
diagbits.4m.t8	60	CSAT3_IRGA_BIN	CSAT3 diagnostic sum, 1=low sig,2=high sig,4=no lock,8=path diff,16=skipped samp
co2.4m.t8	60	CSAT3_IRGA_BIN	CO_2 density from CSI IRGA
h2o.4m.t8	60	CSAT3_IRGA_BIN	Water vapor density from CSI IRGA
irgadiag.4m.t8	60	CSAT3_IRGA_BIN	CSI IRGA diagnostic
Tirga.4m.t8	60	CSAT3_IRGA_BIN	CSI IRGA temperature
Pirga.4m.t8	60	CSAT3_IRGA_BIN	CSI IRGA pressure
ldiag.4m.t8	60	CSAT3_IRGA_BIN	CSAT3 logical diagnostic, 0=OK, 1=(diagbits!=0)
T.4m.t8	1	NCAR_SHT	Air Temperature, NCAR hygro-thermometer
RH.4m.t8	1	NCAR_SHT	Relative Humidity, NCAR hygro-thermometer
P.4m.t8	20	Nano	Barometric Pressure, Paroscientific 6000
u.4m.t9	60	CSAT3A_BIN	Wind U component, CSAT3
v.4m.t9	60	CSAT3A_BIN	Wind V component, CSAT3
w.4m.t9	60	CSAT3A_BIN	Wind W component, CSAT3
tc.4m.t9	60	CSAT3A_BIN	Virtual air temperature from speed of sound, CSAT3
diagbits.4m.t9	60	CSAT3A_BIN	CSAT3 diagnostic sum, 1=low sig,2=high sig,4=no lock,8=path diff,16=skipped samp
ldiag.4m.t9	60	CSAT3A_BIN	CSAT3 logical diagnostic, 0=OK, 1=(diagbits!=0)
u.4m.t10	30	CSAT3	Wind U component, CSAT3
v.4m.t10	30	CSAT3	Wind V component, CSAT3
w.4m.t10	30	CSAT3	Wind W component, CSAT3
tc.4m.t10	30	CSAT3	Virtual air temperature from speed of sound, CSAT3
diagbits.4m.t10	30	CSAT3	CSAT3 diagnostic sum, 1=low sig,2=high sig,4=no lock,8=path diff,16=skipped samp
ldiag.4m.t10	30	CSAT3	CSAT3 logical diagnostic, 0=OK, 1=(diagbits!=0)
u.4m.t11	60	CSAT3_IRGA_BIN	Wind U component, CSAT3
v.4m.t11	60	CSAT3_IRGA_BIN	Wind V component, CSAT3

w.4m.t11	60	CSAT3_IRGA_BIN	Wind W component, CSAT3
tc.4m.t11	60	CSAT3_IRGA_BIN	Virtual air temperature from speed of sound, CSAT3
diagbits.4m.t11	60	CSAT3_IRGA_BIN	CSAT3 diagnostic sum, 1=low sig,2=high sig,4=no lock,8=path diff,16=skipped samp
co2.4m.t11	60	CSAT3_IRGA_BIN	CO_2 density from CSI IRGA
h2o.4m.t11	60	CSAT3_IRGA_BIN	Water vapor density from CSI IRGA
irgadiag.4m.t11	60	CSAT3_IRGA_BIN	CSI IRGA diagnostic
Tirga.4m.t11	60	CSAT3_IRGA_BIN	CSI IRGA temperature
Pirga.4m.t11	60	CSAT3_IRGA_BIN	CSI IRGA pressure
ldiag.4m.t11	60	CSAT3_IRGA_BIN	CSAT3 logical diagnostic, 0=OK, 1=(diagbits!=0)
T.4m.t11	1	NCAR_SHT	Air Temperature, NCAR hygro-thermometer
RH.4m.t11	1	NCAR_SHT	Relative Humidity, NCAR hygro-thermometer
P.4m.t11	20	Nano	Barometric Pressure, Paroscientific 6000
u.4m.t12	50	CSAT3B	Wind U component, CSAT3BH
v.4m.t12	50	CSAT3B	Wind V component, CSAT3BH
w.4m.t12	50	CSAT3B	Wind W component, CSAT3BH
tc.4m.t12	50	CSAT3B	Virtual air temperature from speed of sound, CSAT3BH
diag.4m.t12	50	CSAT3B	CSAT3BH diagnostic sum
ldiag.4m.t12	50	CSAT3B	CSAT3BH logical diagnostic, 0=OK, 1=(diagbits!=0)
u.4m.t13	30	CSAT3	Wind U component, CSAT3
v.4m.t13	30	CSAT3	Wind V component, CSAT3
w.4m.t13	30	CSAT3	Wind W component, CSAT3
tc.4m.t13	30	CSAT3	Virtual air temperature from speed of sound, CSAT3
diagbits.4m.t13	30	CSAT3	CSAT3 diagnostic sum, 1=low sig,2=high sig,4=no lock,8=path diff,16=skipped samp
ldiag.4m.t13	30	CSAT3	CSAT3 logical diagnostic, 0=OK, 1=(diagbits!=0)
u.4m.t14	60	CSAT3_IRGA_BIN	Wind U component, CSAT3
v.4m.t14	60	CSAT3_IRGA_BIN	Wind V component, CSAT3
w.4m.t14	60	CSAT3_IRGA_BIN	Wind W component, CSAT3
tc.4m.t14	60	CSAT3_IRGA_BIN	Virtual air temperature from speed of sound, CSAT3
diagbits.4m.t14	60	CSAT3_IRGA_BIN	CSAT3 diagnostic sum, 1=low sig,2=high sig,4=no lock,8=path diff,16=skipped samp
co2.4m.t14	60	CSAT3_IRGA_BIN	CO_2 density from CSI IRGA
h2o.4m.t14	60	CSAT3_IRGA_BIN	Water vapor density from CSI IRGA
irgadiag.4m.t14	60	CSAT3_IRGA_BIN	CSI IRGA diagnostic
Tirga.4m.t14	60	CSAT3_IRGA_BIN	CSI IRGA temperature
Pirga.4m.t14	60	CSAT3_IRGA_BIN	CSI IRGA pressure
ldiag.4m.t14	60	CSAT3_IRGA_BIN	CSAT3 logical diagnostic, 0=OK, 1=(diagbits!=0)

T.4m.t14	1	NCAR_SHT	Air Temperature, NCAR hygro-thermometer
RH.4m.t14	1	NCAR_SHT	Relative Humidity, NCAR hygro-thermometer
P.4m.t14	20	Nano	Barometric Pressure, Paroscientific 6000
u.4m.t15	60	CSAT3A_BIN	Wind U component, CSAT3
v.4m.t15	60	CSAT3A_BIN	Wind V component, CSAT3
w.4m.t15	60	CSAT3A_BIN	Wind W component, CSAT3
tc.4m.t15	60	CSAT3A_BIN	Virtual air temperature from speed of sound, CSAT3
diagbits.4m.t15	60	CSAT3A_BIN	CSAT3 diagnostic sum, 1=low sig,2=high sig,4=no lock,8=path diff,16=skipped samp
ldiag.4m.t15	60	CSAT3A_BIN	CSAT3 logical diagnostic, 0=OK, 1=(diagbits!=0)
u.4m.t16	30	CSAT3	Wind U component, CSAT3
v.4m.t16	30	CSAT3	Wind V component, CSAT3
w.4m.t16	30	CSAT3	Wind W component, CSAT3
tc.4m.t16	30	CSAT3	Virtual air temperature from speed of sound, CSAT3
diagbits.4m.t16	30	CSAT3	CSAT3 diagnostic sum, 1=low sig,2=high sig,4=no lock,8=path diff,16=skipped samp
ldiag.4m.t16	30	CSAT3	CSAT3 logical diagnostic, 0=OK, 1=(diagbits!=0)
u.4m.t17	60	CSAT3_IRGA_BIN	Wind U component, CSAT3
v.4m.t17	60	CSAT3_IRGA_BIN	Wind V component, CSAT3
w.4m.t17	60	CSAT3_IRGA_BIN	Wind W component, CSAT3
tc.4m.t17	60	CSAT3_IRGA_BIN	Virtual air temperature from speed of sound, CSAT3
diagbits.4m.t17	60	CSAT3_IRGA_BIN	CSAT3 diagnostic sum, 1=low sig,2=high sig,4=no lock,8=path diff,16=skipped samp
co2.4m.t17	60	CSAT3_IRGA_BIN	CO_2 density from CSI IRGA
h2o.4m.t17	60	CSAT3_IRGA_BIN	Water vapor density from CSI IRGA
irgadiag.4m.t17	60	CSAT3_IRGA_BIN	CSI IRGA diagnostic
Tirga.4m.t17	60	CSAT3_IRGA_BIN	CSI IRGA temperature
Pirga.4m.t17	60	CSAT3_IRGA_BIN	CSI IRGA pressure
ldiag.4m.t17	60	CSAT3_IRGA_BIN	CSAT3 logical diagnostic, 0=OK, 1=(diagbits!=0)
T.4m.t17	1	NCAR_SHT	Air Temperature, NCAR hygro-thermometer
RH.4m.t17	1	NCAR_SHT	Relative Humidity, NCAR hygro-thermometer
P.4m.t17	20	Nano	Barometric Pressure, Paroscientific 6000
u.4m.t18	50	CSAT3B	Wind U component, CSAT3BH
v.4m.t18	50	CSAT3B	Wind V component, CSAT3BH
w.4m.t18	50	CSAT3B	Wind W component, CSAT3BH
tc.4m.t18	50	CSAT3B	Virtual air temperature from speed of sound, CSAT3BH
diag.4m.t18	50	CSAT3B	CSAT3BH diagnostic sum
ldiag.4m.t18	50	CSAT3B	CSAT3BH logical diagnostic, 0=OK, 1=(diagbits!=0)

u.4m.t19	30	CSAT3	Wind U component, CSAT3
v.4m.t19	30	CSAT3	Wind V component, CSAT3
w.4m.t19	30	CSAT3	Wind W component, CSAT3
tc.4m.t19	30	CSAT3	Virtual air temperature from speed of sound, CSAT3
diagbits.4m.t19	30	CSAT3	CSAT3 diagnostic sum, 1=low sig,2=high sig,4=no lock,8=path diff,16=skipped samp
ldiag.4m.t19	30	CSAT3	CSAT3 logical diagnostic, 0=OK, 1=(diagbits!=0)
u.4m.t20	60	CSAT3_IRGA_BIN	Wind U component, CSAT3
v.4m.t20	60	CSAT3_IRGA_BIN	Wind V component, CSAT3
w.4m.t20	60	CSAT3_IRGA_BIN	Wind W component, CSAT3
tc.4m.t20	60	CSAT3_IRGA_BIN	Virtual air temperature from speed of sound, CSAT3
diagbits.4m.t20	60	CSAT3_IRGA_BIN	CSAT3 diagnostic sum, 1=low sig,2=high sig,4=no lock,8=path diff,16=skipped samp
co2.4m.t20	60	CSAT3_IRGA_BIN	CO_2 density from CSI IRGA
h2o.4m.t20	60	CSAT3_IRGA_BIN	Water vapor density from CSI IRGA
irgadiag.4m.t20	60	CSAT3_IRGA_BIN	CSI IRGA diagnostic
Tirga.4m.t20	60	CSAT3_IRGA_BIN	CSI IRGA temperature
Pirga.4m.t20	60	CSAT3_IRGA_BIN	CSI IRGA pressure
ldiag.4m.t20	60	CSAT3_IRGA_BIN	CSAT3 logical diagnostic, 0=OK, 1=(diagbits!=0)
T.4m.t20	1	NCAR_SHT	Air Temperature, NCAR hygro-thermometer
RH.4m.t20	1	NCAR_SHT	Relative Humidity, NCAR hygro-thermometer
P.4m.t20	20	Nano	Barometric Pressure, Paroscientific 6000
u.4m.t21	60	CSAT3A_BIN	Wind U component, CSAT3
v.4m.t21	60	CSAT3A_BIN	Wind V component, CSAT3
w.4m.t21	60	CSAT3A_BIN	Wind W component, CSAT3
tc.4m.t21	60	CSAT3A_BIN	Virtual air temperature from speed of sound, CSAT3
diagbits.4m.t21	60	CSAT3A_BIN	CSAT3 diagnostic sum, 1=low sig,2=high sig,4=no lock,8=path diff,16=skipped samp
ldiag.4m.t21	60	CSAT3A_BIN	CSAT3 logical diagnostic, 0=OK, 1=(diagbits!=0)
u.4m.t22	30	CSAT3	Wind U component, CSAT3
v.4m.t22	30	CSAT3	Wind V component, CSAT3
w.4m.t22	30	CSAT3	Wind W component, CSAT3
tc.4m.t22	30	CSAT3	Virtual air temperature from speed of sound, CSAT3
diagbits.4m.t22	30	CSAT3	CSAT3 diagnostic sum, 1=low sig,2=high sig,4=no lock,8=path diff,16=skipped samp
ldiag.4m.t22	30	CSAT3	CSAT3 logical diagnostic, 0=OK, 1=(diagbits!=0)
u.4m.t23	60	CSAT3_IRGA_BIN	Wind U component, CSAT3
v.4m.t23	60	CSAT3_IRGA_BIN	Wind V component, CSAT3

w.4m.t23	60	CSAT3_IRGA_BIN	Wind W component, CSAT3
tc.4m.t23	60	CSAT3_IRGA_BIN	Virtual air temperature from speed of sound, CSAT3
diagbits.4m.t23	60	CSAT3_IRGA_BIN	CSAT3 diagnostic sum, 1=low sig,2=high sig,4=no lock,8=path diff,16=skipped samp
co2.4m.t23	60	CSAT3_IRGA_BIN	CO_2 density from CSI IRGA
h2o.4m.t23	60	CSAT3_IRGA_BIN	Water vapor density from CSI IRGA
irgadiag.4m.t23	60	CSAT3_IRGA_BIN	CSI IRGA diagnostic
Tirga.4m.t23	60	CSAT3_IRGA_BIN	CSI IRGA temperature
Pirga.4m.t23	60	CSAT3_IRGA_BIN	CSI IRGA pressure
ldiag.4m.t23	60	CSAT3_IRGA_BIN	CSAT3 logical diagnostic, 0=OK, 1=(diagbits!=0)
T.4m.t23	1	NCAR_SHT	Air Temperature, NCAR hygro-thermometer
RH.4m.t23	1	NCAR_SHT	Relative Humidity, NCAR hygro-thermometer
P.4m.t23	20	Nano	Barometric Pressure, Paroscientific 6000
u.4m.t24	50	CSAT3B	Wind U component, CSAT3BH
v.4m.t24	50	CSAT3B	Wind V component, CSAT3BH
w.4m.t24	50	CSAT3B	Wind W component, CSAT3BH
tc.4m.t24	50	CSAT3B	Virtual air temperature from speed of sound, CSAT3BH
diag.4m.t24	50	CSAT3B	CSAT3BH diagnostic sum
ldiag.4m.t24	50	CSAT3B	CSAT3BH logical diagnostic, 0=OK, 1=(diagbits!=0)
u.4m.t25	30	CSAT3	Wind U component, CSAT3
v.4m.t25	30	CSAT3	Wind V component, CSAT3
w.4m.t25	30	CSAT3	Wind W component, CSAT3
tc.4m.t25	30	CSAT3	Virtual air temperature from speed of sound, CSAT3
diagbits.4m.t25	30	CSAT3	CSAT3 diagnostic sum, 1=low sig,2=high sig,4=no lock,8=path diff,16=skipped samp
ldiag.4m.t25	30	CSAT3	CSAT3 logical diagnostic, 0=OK, 1=(diagbits!=0)
u.4m.t26	60	CSAT3_IRGA_BIN	Wind U component, CSAT3
v.4m.t26	60	CSAT3_IRGA_BIN	Wind V component, CSAT3
w.4m.t26	60	CSAT3_IRGA_BIN	Wind W component, CSAT3
tc.4m.t26	60	CSAT3_IRGA_BIN	Virtual air temperature from speed of sound, CSAT3
diagbits.4m.t26	60	CSAT3_IRGA_BIN	CSAT3 diagnostic sum, 1=low sig,2=high sig,4=no lock,8=path diff,16=skipped samp
co2.4m.t26	60	CSAT3_IRGA_BIN	CO_2 density from CSI IRGA
h2o.4m.t26	60	CSAT3_IRGA_BIN	Water vapor density from CSI IRGA
irgadiag.4m.t26	60	CSAT3_IRGA_BIN	CSI IRGA diagnostic
Tirga.4m.t26	60	CSAT3_IRGA_BIN	CSI IRGA temperature
Pirga.4m.t26	60	CSAT3_IRGA_BIN	CSI IRGA pressure
ldiag.4m.t26	60	CSAT3_IRGA_BIN	CSAT3 logical diagnostic, 0=OK, 1=(diagbits!=0)

T.4m.t26	1	NCAR_SHT	Air Temperature, NCAR hygro-thermometer
RH.4m.t26	1	NCAR_SHT	Relative Humidity, NCAR hygro-thermometer
P.4m.t26	20	Nano	Barometric Pressure, Paroscientific 6000
u.4m.t27	60	CSAT3A_BIN	Wind U component, CSAT3
v.4m.t27	60	CSAT3A_BIN	Wind V component, CSAT3
w.4m.t27	60	CSAT3A_BIN	Wind W component, CSAT3
tc.4m.t27	60	CSAT3A_BIN	Virtual air temperature from speed of sound, CSAT3
diagbits.4m.t27	60	CSAT3A_BIN	CSAT3 diagnostic sum, 1=low sig,2=high sig,4=no lock,8=path diff,16=skipped samp
ldiag.4m.t27	60	CSAT3A_BIN	CSAT3 logical diagnostic, 0=OK, 1=(diagbits!=0)
u.4m.t28	30	CSAT3	Wind U component, CSAT3
v.4m.t28	30	CSAT3	Wind V component, CSAT3
w.4m.t28	30	CSAT3	Wind W component, CSAT3
tc.4m.t28	30	CSAT3	Virtual air temperature from speed of sound, CSAT3
diagbits.4m.t28	30	CSAT3	CSAT3 diagnostic sum, 1=low sig,2=high sig,4=no lock,8=path diff,16=skipped samp
ldiag.4m.t28	30	CSAT3	CSAT3 logical diagnostic, 0=OK, 1=(diagbits!=0)
u.4m.t29	60	CSAT3_IRGA_BIN	Wind U component, CSAT3
v.4m.t29	60	CSAT3_IRGA_BIN	Wind V component, CSAT3
w.4m.t29	60	CSAT3_IRGA_BIN	Wind W component, CSAT3
tc.4m.t29	60	CSAT3_IRGA_BIN	Virtual air temperature from speed of sound, CSAT3
diagbits.4m.t29	60	CSAT3_IRGA_BIN	CSAT3 diagnostic sum, 1=low sig,2=high sig,4=no lock,8=path diff,16=skipped samp
co2.4m.t29	60	CSAT3_IRGA_BIN	CO_2 density from CSI IRGA
h2o.4m.t29	60	CSAT3_IRGA_BIN	Water vapor density from CSI IRGA
irgadiag.4m.t29	60	CSAT3_IRGA_BIN	CSI IRGA diagnostic
Tirga.4m.t29	60	CSAT3_IRGA_BIN	CSI IRGA temperature
Pirga.4m.t29	60	CSAT3_IRGA_BIN	CSI IRGA pressure
ldiag.4m.t29	60	CSAT3_IRGA_BIN	CSAT3 logical diagnostic, 0=OK, 1=(diagbits!=0)
T.4m.t29	1	NCAR_SHT	Air Temperature, NCAR hygro-thermometer
RH.4m.t29	1	NCAR_SHT	Relative Humidity, NCAR hygro-thermometer
P.4m.t29	20	Nano	Barometric Pressure, Paroscientific 6000
u.4m.t30	50	CSAT3B	Wind U component, CSAT3BH
v.4m.t30	50	CSAT3B	Wind V component, CSAT3BH
w.4m.t30	50	CSAT3B	Wind W component, CSAT3BH
tc.4m.t30	50	CSAT3B	Virtual air temperature from speed of sound, CSAT3BH
diag.4m.t30	50	CSAT3B	CSAT3BH diagnostic sum
ldiag.4m.t30	50	CSAT3B	CSAT3BH logical diagnostic, 0=OK, 1=(diagbits!=0)

u.4m.t31	30	CSAT3	Wind U component, CSAT3
v.4m.t31	30	CSAT3	Wind V component, CSAT3
w.4m.t31	30	CSAT3	Wind W component, CSAT3
tc.4m.t31	30	CSAT3	Virtual air temperature from speed of sound, CSAT3
diagbits.4m.t31	30	CSAT3	CSAT3 diagnostic sum, 1=low sig,2=high sig,4=no lock,8=path diff,16=skipped samp
ldiag.4m.t31	30	CSAT3	CSAT3 logical diagnostic, 0=OK, 1=(diagbits!=0)
u.4m.t32	60	CSAT3_IRGA_BIN	Wind U component, CSAT3
v.4m.t32	60	CSAT3_IRGA_BIN	Wind V component, CSAT3
w.4m.t32	60	CSAT3_IRGA_BIN	Wind W component, CSAT3
tc.4m.t32	60	CSAT3_IRGA_BIN	Virtual air temperature from speed of sound, CSAT3
diagbits.4m.t32	60	CSAT3_IRGA_BIN	CSAT3 diagnostic sum, 1=low sig,2=high sig,4=no lock,8=path diff,16=skipped samp
co2.4m.t32	60	CSAT3_IRGA_BIN	CO_2 density from CSI IRGA
h2o.4m.t32	60	CSAT3_IRGA_BIN	Water vapor density from CSI IRGA
irgadiag.4m.t32	60	CSAT3_IRGA_BIN	CSI IRGA diagnostic
Tirga.4m.t32	60	CSAT3_IRGA_BIN	CSI IRGA temperature
Pirga.4m.t32	60	CSAT3_IRGA_BIN	CSI IRGA pressure
ldiag.4m.t32	60	CSAT3_IRGA_BIN	CSAT3 logical diagnostic, 0=OK, 1=(diagbits!=0)
T.4m.t32	1	NCAR_SHT	Air Temperature, NCAR hygro-thermometer
RH.4m.t32	1	NCAR_SHT	Relative Humidity, NCAR hygro-thermometer
P.4m.t32	20	Nano	Barometric Pressure, Paroscientific 6000
u.4m.t33	30	CSAT3	Wind U component, CSAT3
v.4m.t33	30	CSAT3	Wind V component, CSAT3
w.4m.t33	30	CSAT3	Wind W component, CSAT3
tc.4m.t33	30	CSAT3	Virtual air temperature from speed of sound, CSAT3
diagbits.4m.t33	30	CSAT3	CSAT3 diagnostic sum, 1=low sig,2=high sig,4=no lock,8=path diff,16=skipped samp
ldiag.4m.t33	30	CSAT3	CSAT3 logical diagnostic, 0=OK, 1=(diagbits!=0)
u.4m.t34	30	CSAT3	Wind U component, CSAT3
v.4m.t34	30	CSAT3	Wind V component, CSAT3
w.4m.t34	30	CSAT3	Wind W component, CSAT3
tc.4m.t34	30	CSAT3	Virtual air temperature from speed of sound, CSAT3
diagbits.4m.t34	30	CSAT3	CSAT3 diagnostic sum, 1=low sig,2=high sig,4=no lock,8=path diff,16=skipped samp
ldiag.4m.t34	30	CSAT3	CSAT3 logical diagnostic, 0=OK, 1=(diagbits!=0)
u.4m.t35	60	CSAT3_IRGA_BIN	Wind U component, CSAT3
v.4m.t35	60	CSAT3_IRGA_BIN	Wind V component, CSAT3

w.4m.t35	60	CSAT3_IRGA_BIN	Wind W component, CSAT3
tc.4m.t35	60	CSAT3_IRGA_BIN	Virtual air temperature from speed of sound, CSAT3
diagbits.4m.t35	60	CSAT3_IRGA_BIN	CSAT3 diagnostic sum, 1=low sig,2=high sig,4=no lock,8=path diff,16=skipped samp
co2.4m.t35	60	CSAT3_IRGA_BIN	CO_2 density from CSI IRGA
h2o.4m.t35	60	CSAT3_IRGA_BIN	Water vapor density from CSI IRGA
irgadiag.4m.t35	60	CSAT3_IRGA_BIN	CSI IRGA diagnostic
Tirga.4m.t35	60	CSAT3_IRGA_BIN	CSI IRGA temperature
Pirga.4m.t35	60	CSAT3_IRGA_BIN	CSI IRGA pressure
ldiag.4m.t35	60	CSAT3_IRGA_BIN	CSAT3 logical diagnostic, 0=OK, 1=(diagbits!=0)
T.4m.t35	1	NCAR_SHT	Air Temperature, NCAR hygro-thermometer
RH.4m.t35	1	NCAR_SHT	Relative Humidity, NCAR hygro-thermometer
P.4m.t35	20	Nano	Barometric Pressure, Paroscientific 6000
u.4m.t36	50	CSAT3B	Wind U component, CSAT3BH
v.4m.t36	50	CSAT3B	Wind V component, CSAT3BH
w.4m.t36	50	CSAT3B	Wind W component, CSAT3BH
tc.4m.t36	50	CSAT3B	Virtual air temperature from speed of sound, CSAT3BH
diag.4m.t36	50	CSAT3B	CSAT3BH diagnostic sum
ldiag.4m.t36	50	CSAT3B	CSAT3BH logical diagnostic, 0=OK, 1=(diagbits!=0)
u.4m.t37	30	CSAT3	Wind U component, CSAT3
v.4m.t37	30	CSAT3	Wind V component, CSAT3
w.4m.t37	30	CSAT3	Wind W component, CSAT3
tc.4m.t37	30	CSAT3	Virtual air temperature from speed of sound, CSAT3
diagbits.4m.t37	30	CSAT3	CSAT3 diagnostic sum, 1=low sig,2=high sig,4=no lock,8=path diff,16=skipped samp
ldiag.4m.t37	30	CSAT3	CSAT3 logical diagnostic, 0=OK, 1=(diagbits!=0)
u.4m.t38	60	CSAT3_IRGA_BIN	Wind U component, CSAT3
v.4m.t38	60	CSAT3_IRGA_BIN	Wind V component, CSAT3
w.4m.t38	60	CSAT3_IRGA_BIN	Wind W component, CSAT3
tc.4m.t38	60	CSAT3_IRGA_BIN	Virtual air temperature from speed of sound, CSAT3
diagbits.4m.t38	60	CSAT3_IRGA_BIN	CSAT3 diagnostic sum, 1=low sig,2=high sig,4=no lock,8=path diff,16=skipped samp
co2.4m.t38	60	CSAT3_IRGA_BIN	CO_2 density from CSI IRGA
h2o.4m.t38	60	CSAT3_IRGA_BIN	Water vapor density from CSI IRGA
irgadiag.4m.t38	60	CSAT3_IRGA_BIN	CSI IRGA diagnostic
Tirga.4m.t38	60	CSAT3_IRGA_BIN	CSI IRGA temperature
Pirga.4m.t38	60	CSAT3_IRGA_BIN	CSI IRGA pressure
ldiag.4m.t38	60	CSAT3_IRGA_BIN	CSAT3 logical diagnostic, 0=OK, 1=(diagbits!=0)

T.4m.t38	1	NCAR_SHT	Air Temperature, NCAR hygro-thermometer
RH.4m.t38	1	NCAR_SHT	Relative Humidity, NCAR hygro-thermometer
P.4m.t38	20	Nano	Barometric Pressure, Paroscientific 6000
u.4m.t39	30	CSAT3	Wind U component, CSAT3
v.4m.t39	30	CSAT3	Wind V component, CSAT3
w.4m.t39	30	CSAT3	Wind W component, CSAT3
tc.4m.t39	30	CSAT3	Virtual air temperature from speed of sound, CSAT3
diagbits.4m.t39	30	CSAT3	CSAT3 diagnostic sum, 1=low sig,2=high sig,4=no lock,8=path diff,16=skipped samp
ldiag.4m.t39	30	CSAT3	CSAT3 logical diagnostic, 0=OK, 1=(diagbits!=0)
u.4m.t40	30	CSAT3	Wind U component, CSAT3
v.4m.t40	30	CSAT3	Wind V component, CSAT3
w.4m.t40	30	CSAT3	Wind W component, CSAT3
tc.4m.t40	30	CSAT3	Virtual air temperature from speed of sound, CSAT3
diagbits.4m.t40	30	CSAT3	CSAT3 diagnostic sum, 1=low sig,2=high sig,4=no lock,8=path diff,16=skipped samp
ldiag.4m.t40	30	CSAT3	CSAT3 logical diagnostic, 0=OK, 1=(diagbits!=0)
u.4m.t41	60	CSAT3_IRGA_BIN	Wind U component, CSAT3
v.4m.t41	60	CSAT3_IRGA_BIN	Wind V component, CSAT3
w.4m.t41	60	CSAT3_IRGA_BIN	Wind W component, CSAT3
tc.4m.t41	60	CSAT3_IRGA_BIN	Virtual air temperature from speed of sound, CSAT3
diagbits.4m.t41	60	CSAT3_IRGA_BIN	CSAT3 diagnostic sum, 1=low sig,2=high sig,4=no lock,8=path diff,16=skipped samp
co2.4m.t41	60	CSAT3_IRGA_BIN	CO_2 density from CSI IRGA
h2o.4m.t41	60	CSAT3_IRGA_BIN	Water vapor density from CSI IRGA
irgadiag.4m.t41	60	CSAT3_IRGA_BIN	CSI IRGA diagnostic
Tirga.4m.t41	60	CSAT3_IRGA_BIN	CSI IRGA temperature
Pirga.4m.t41	60	CSAT3_IRGA_BIN	CSI IRGA pressure
ldiag.4m.t41	60	CSAT3_IRGA_BIN	CSAT3 logical diagnostic, 0=OK, 1=(diagbits!=0)
T.4m.t41	1	NCAR_SHT	Air Temperature, NCAR hygro-thermometer
RH.4m.t41	1	NCAR_SHT	Relative Humidity, NCAR hygro-thermometer
P.4m.t41	20	Nano	Barometric Pressure, Paroscientific 6000
u.4m.t42	50	CSAT3B	Wind U component, CSAT3BH
v.4m.t42	50	CSAT3B	Wind V component, CSAT3BH
w.4m.t42	50	CSAT3B	Wind W component, CSAT3BH
tc.4m.t42	50	CSAT3B	Virtual air temperature from speed of sound, CSAT3BH
diag.4m.t42	50	CSAT3B	CSAT3BH diagnostic sum
ldiag.4m.t42	50	CSAT3B	CSAT3BH logical diagnostic, 0=OK, 1=(diagbits!=0)

u.4m.t43	30	CSAT3	Wind U component, CSAT3
v.4m.t43	30	CSAT3	Wind V component, CSAT3
w.4m.t43	30	CSAT3	Wind W component, CSAT3
tc.4m.t43	30	CSAT3	Virtual air temperature from speed of sound, CSAT3
diagbits.4m.t43	30	CSAT3	CSAT3 diagnostic sum, 1=low sig,2=high sig,4=no lock,8=path diff,16=skipped samp
ldiag.4m.t43	30	CSAT3	CSAT3 logical diagnostic, 0=OK, 1=(diagbits!=0)
u.4m.t44	60	CSAT3_IRGA_BIN	Wind U component, CSAT3
v.4m.t44	60	CSAT3_IRGA_BIN	Wind V component, CSAT3
w.4m.t44	60	CSAT3_IRGA_BIN	Wind W component, CSAT3
tc.4m.t44	60	CSAT3_IRGA_BIN	Virtual air temperature from speed of sound, CSAT3
diagbits.4m.t44	60	CSAT3_IRGA_BIN	CSAT3 diagnostic sum, 1=low sig,2=high sig,4=no lock,8=path diff,16=skipped samp
co2.4m.t44	60	CSAT3_IRGA_BIN	CO_2 density from CSI IRGA
h2o.4m.t44	60	CSAT3_IRGA_BIN	Water vapor density from CSI IRGA
irgadiag.4m.t44	60	CSAT3_IRGA_BIN	CSI IRGA diagnostic
Tirga.4m.t44	60	CSAT3_IRGA_BIN	CSI IRGA temperature
Pirga.4m.t44	60	CSAT3_IRGA_BIN	CSI IRGA pressure
ldiag.4m.t44	60	CSAT3_IRGA_BIN	CSAT3 logical diagnostic, 0=OK, 1=(diagbits!=0)
T.4m.t44	1	NCAR_SHT	Air Temperature, NCAR hygro-thermometer
RH.4m.t44	1	NCAR_SHT	Relative Humidity, NCAR hygro-thermometer
P.4m.t44	20	Nano	Barometric Pressure, Paroscientific 6000
u.4m.t45	30	CSAT3	Wind U component, CSAT3
v.4m.t45	30	CSAT3	Wind V component, CSAT3
w.4m.t45	30	CSAT3	Wind W component, CSAT3
tc.4m.t45	30	CSAT3	Virtual air temperature from speed of sound, CSAT3
diagbits.4m.t45	30	CSAT3	CSAT3 diagnostic sum, 1=low sig,2=high sig,4=no lock,8=path diff,16=skipped samp
ldiag.4m.t45	30	CSAT3	CSAT3 logical diagnostic, 0=OK, 1=(diagbits!=0)
u.4m.t46	30	CSAT3	Wind U component, CSAT3
v.4m.t46	30	CSAT3	Wind V component, CSAT3
w.4m.t46	30	CSAT3	Wind W component, CSAT3
tc.4m.t46	30	CSAT3	Virtual air temperature from speed of sound, CSAT3
diagbits.4m.t46	30	CSAT3	CSAT3 diagnostic sum, 1=low sig,2=high sig,4=no lock,8=path diff,16=skipped samp
ldiag.4m.t46	30	CSAT3	CSAT3 logical diagnostic, 0=OK, 1=(diagbits!=0)
u.4m.t47	60	CSAT3_IRGA_BIN	Wind U component, CSAT3
v.4m.t47	60	CSAT3_IRGA_BIN	Wind V component, CSAT3

w.4m.t47	60	CSAT3_IRGA_BIN	Wind W component, CSAT3
tc.4m.t47	60	CSAT3_IRGA_BIN	Virtual air temperature from speed of sound, CSAT3
diagbits.4m.t47	60	CSAT3_IRGA_BIN	CSAT3 diagnostic sum, 1=low sig,2=high sig,4=no lock,8=path diff,16=skipped samp
co2.4m.t47	60	CSAT3_IRGA_BIN	CO_2 density from CSI IRGA
h2o.4m.t47	60	CSAT3_IRGA_BIN	Water vapor density from CSI IRGA
irgadiag.4m.t47	60	CSAT3_IRGA_BIN	CSI IRGA diagnostic
Tirga.4m.t47	60	CSAT3_IRGA_BIN	CSI IRGA temperature
Pirga.4m.t47	60	CSAT3_IRGA_BIN	CSI IRGA pressure
ldiag.4m.t47	60	CSAT3_IRGA_BIN	CSAT3 logical diagnostic, 0=OK, 1=(diagbits!=0)
T.4m.t47	1	NCAR_SHT	Air Temperature, NCAR hygro-thermometer
RH.4m.t47	1	NCAR_SHT	Relative Humidity, NCAR hygro-thermometer
P.4m.t47	20	Nano	Barometric Pressure, Paroscientific 6000
u.4m.t48	50	CSAT3B	Wind U component, CSAT3BH
v.4m.t48	50	CSAT3B	Wind V component, CSAT3BH
w.4m.t48	50	CSAT3B	Wind W component, CSAT3BH
tc.4m.t48	50	CSAT3B	Virtual air temperature from speed of sound, CSAT3BH
diag.4m.t48	50	CSAT3B	CSAT3BH diagnostic sum
ldiag.4m.t48	50	CSAT3B	CSAT3BH logical diagnostic, 0=OK, 1=(diagbits!=0)
u.4m.t49	30	CSAT3	Wind U component, CSAT3
v.4m.t49	30	CSAT3	Wind V component, CSAT3
w.4m.t49	30	CSAT3	Wind W component, CSAT3
tc.4m.t49	30	CSAT3	Virtual air temperature from speed of sound, CSAT3
diagbits.4m.t49	30	CSAT3	CSAT3 diagnostic sum, 1=low sig,2=high sig,4=no lock,8=path diff,16=skipped samp
ldiag.4m.t49	30	CSAT3	CSAT3 logical diagnostic, 0=OK, 1=(diagbits!=0)